

# Catastrophic caldera-forming pyroclastic eruptions and climate perturbations: the result of tectonic and magmatic controls on the Paleocene-Eocene Kilchrist Caldera, Isle of Skye, NW Scotland

Simon M. Drake\*<sup>α</sup>,  David J. Brown<sup>β</sup>,  Andrew D. Beard<sup>α</sup>, Padej Kumlersakul<sup>α</sup>, David J. Thompson<sup>α</sup>,  Charlotte L. Bays<sup>α</sup>,  Ian L. Millar<sup>γ</sup>, and  Kathryn M. Goodenough<sup>δ</sup>

<sup>α</sup> School of Earth and Planetary Sciences, Birkbeck College, University of London, Malet St, London, WC1E 7HX, UK.

<sup>β</sup> School of Geographical and Earth Sciences, University of Glasgow, Lilybank Gardens, Glasgow, G12 8QQ, UK.

<sup>γ</sup> British Geological Survey, Natural Environment Research Council, Keyworth, Nottingham, NG12 5GC, UK.

<sup>δ</sup> British Geological Survey, Research Avenue South, Edinburgh, EH14 4AP, UK.

## ABSTRACT

Caldera-forming eruptions are amongst the most hazardous events in the Earth's history. In this study we present new evidence for a Paleocene-Eocene caldera from Skye, NW Scotland. Magma exploited a Palaeozoic regional thrust fault zone and Mesozoic strata, and ponded against a 'barrier' of intrusive igneous rocks emplaced against a regional extensional fault. Replenishment of silicic magma reservoirs with basaltic magma triggered eruptions. The eruptions typically deposited coarse ignimbrites, demonstrating catastrophic collapse of the caldera, which occurred via an inner ring-fault and a complexly faulted margin. Collapse was followed by remobilisation of silicic magma and caldera resurgence. Magma induced dissociation in dolostone, and dehydration and cracking of organic-rich country rocks via contact metamorphism. This caused a significant release of CO<sub>2</sub> and CH<sub>4</sub>, which contributed to the Paleocene-Eocene Thermal Maximum. Our results demonstrate how tectonics localise magma and calderas, and how this can cause cataclysmic volcanic and climatic hazards.

KEYWORDS: Caldera; Ignimbrite; PETM; Tectonics; Skye.

## 1 INTRODUCTION

The influence of both regional-scale reverse and normal faults, and large-scale solidified igneous intrusions on magma migration pathways and caldera morphology is largely unknown. Whilst modelling studies show that both basic and silicic magma can preferentially exploit pre-existing thrust fault ramps and flats [Ferré et al. 2012], real examples are lacking. The influence of regional-scale extension on caldera development has largely been determined by analogue modelling, which indicates both local crustal extension and magma chamber overpressure can promote high-mass-flux, dyke-fed eruptions [Costa et al. 2011]. Whilst it is known that minor intrusions can act as both barriers and conduits to fluid migration [Rateau et al. 2013], the effect of large-scale solidified intrusive centres on magma migration, caldera development, and morphology remains unknown. Large silicic eruptions also emit aerosols and gases which may include sulphuric acid (H<sub>2</sub>SO<sub>4</sub>), which causes atmospheric cooling, together with carbon dioxide (CO<sub>2</sub>) and methane (CH<sub>4</sub>), which both cause global warming [Ganino and Arndt 2009]. The release of CO<sub>2</sub> and CH<sub>4</sub> due to emplacement of magma into country rocks can also contribute significantly to climate change.

In this study we detail a Paleocene caldera (Figures 1 and 2) at Kilchrist, Skye, whose morphology was constrained by solidified intrusive barriers to its north. Magma was transported via a pre-existing, inert, regional-scale thrust fault zone to its south. As the caldera grew, magma ponded against the barriers. Subsequent caldera collapse within an inner ring-fault,

led to development of a complex multiple-block faulted outer margin, and produced coarse lithic lapilli- and block-rich ignimbrites. Throughout eruptions, magma chamber replenishments of mafic melt took place, which likely acted as eruption triggers. Contemporaneous regional-scale extension created vertical fissures within the caldera, through which silicic magma ascended and erupted at the surface, feeding pyroclastic density currents (PDCs) that deposited lava-like and welded ignimbrites. We have identified four distinct eruption stages within the caldera. Throughout the volcanic, and subsequent resurgent intrusive episode, decarbonation of significant amounts of Cambro-Ordovician dolostone and dehydration of organic-rich Lower Jurassic mudstones and shales by contact metamorphism, released substantial quantities of CO<sub>2</sub> and CH<sub>4</sub> into the atmosphere. We suggest this probably contributed significantly to the Paleocene Eocene Thermal Maximum (PETM).

## 2 GEOLOGICAL SETTING

### 2.1 Pre-Paleocene geology of Skye

The pre-Paleocene geology of the Isle of Skye is highly complex and variable (Figures 1 and 2). The SE of the island is dominated by Archaean-Mesoproterozoic Lewisian Gneiss Complex metamorphic 'basement', Neoproterozoic Sleaf and Torridon Group sedimentary rocks, Neoproterozoic Moine Supergroup meta-sedimentary rocks, and Cambro-Ordovician sedimentary rocks [Bell and Harris 1986; Emeleus and Bell 2005]. The field relationships of these different units have been complicated by thrusting events during the Caledonian

Orogeny in the Silurian. The Lewisian, Torridon, and Moine rocks were thrust over a foreland comprising the same lithologies and the Cambro-Ordovician strata. Collectively the thrust faults form part of the Moine Thrust Zone and include the associated Kishorn Thrust in the study area [Coward and Whalley 1979; Potts 1993] (Figures 2 and 3). The basement Lewisian comprises felsic and mafic banded gneiss. In the foreland succession (footwall), the sedimentary rocks of the Torridon Group comprise the lowermost Diabaig Formation, overlain by the dominant Applecross Formation and its characteristic red-brown sandstone, and finally the Aultbea Formation. In the Kishorn Thrust Sheet succession (hanging wall), the Sleaf Group is overlain by the Torridon Group Applecross Formation. The Moine Supergroup rocks comprise psammite and pelite. The Cambro-Ordovician rocks of the foreland comprise sandstones of the Eriboll Formation and An t-Stron Formation and various dolostones of the Durness Group, which crop out widely in the study area. [BGS 2005]. The majority of the remainder of the island comprises Mesozoic sedimentary rocks overlain by Paleocene basaltic lavas as well as Paleocene intrusive igneous rocks of the Skye Central Complex (see below). Triassic rocks comprise minor sedimentary exposures of the Stornoway Formation whilst Jurassic rocks comprise several hundred metres thickness of sandstone, mudstone, and limestone. In the main study area, key lithologies comprise Lower Jurassic sandstone and siltstone of the Breakish Formation, the Ardnish Formation and the 'Broadford Beds', and mudstone of the Pabay Shale Formation and Middle Jurassic exposures of the Bearreraig Sandstone Formation and the Great Estuarine Group. Very thin exposures of Upper Cretaceous sandstone are locally preserved.

## 2.2 Palaeocene geology of Skye

The Palaeocene geology of the Isle of Skye forms part of the North Atlantic Igneous Province (NAIP; Figure 1A), a Paleocene Large Igneous Province dominated by basaltic lavas, intrusions, and greatly subordinate pyroclastic, volcanoclastic, and sedimentary rocks [Saunders et al. 1997]. Within the NAIP is the much smaller British Paleogene Igneous Province (BPIP) which spans the Inner Hebrides, NW Scotland, and NE Northern Ireland/Ireland (Figure 1B and C). The BPIP comprises extensive lava fields on Skye, Eigg, Mull, and Antrim [Emeleus and Bell 2005]. These lava fields were fissure-fed and associated with a NNW-SSE-trending regional dyke swarm linked to North Atlantic extension [England 1988]. Intrusive central complexes on Ardnamurchan, Arran, Mull, Rum, and Skye in Scotland, and Carlingford, the Mourne, and Slieve Gullion in Northern Ireland/Ireland cut the lava fields [Emeleus and Bell 2005]. Regional dykes are emplaced throughout the lava fields and central complexes. Whilst much BPIP research has concentrated on the gabbroic and granitic central complexes (Figure 1B–D) together with the basaltic lava fields [Bell 1966; 1976; Bell and Williamson 1994; Williamson and Bell 1994; Goultly et al. 1996], less attention has been paid to silicic volcanic rocks. However, detailed mapping, logging, and re-interpretation of silicic volcanic sequences has recently been conducted on Eigg [Brown and Bell 2013], Skye [Drake and Beard 2012], Arran [Gooday et al. 2018],

and Rum [Holohan et al. 2009; Troll et al. 2020]. Apart from deposits found on Eigg and Northern Ireland, all silicic ignimbrites found in the BPIP are associated with either caldera collapse, ring dykes, or both.

Short-lived Paleocene volcanism/magmatism on Skye took place between  $\sim 61.54 \pm 0.42$  Ma [Hamilton et al. 1998; Drake et al. 2017] and  $55.7 \pm 0.1$  Ma [M. A. Hamilton, in Emeleus and Bell 2005] and may have been driven by meteorite impact allied to the  $61.54 \pm 0.42$ – $60 \pm 0.23$  Ma meteoritic ejecta layer, recently reported from Skye [Drake et al. 2017]. The Skye Lava Group dominates Skye's Paleocene geology [Harker and Clough 1904; Williamson and Bell 1994] (Figure 1D), and is cut by the Skye Central Complex which comprises intrusive and volcanic units. These have been subdivided, in age of emplacement from oldest to youngest, into the Cuillin Centre, the Srath na Creitheach Centre, the Western Red Hills (WRH) Centre, and the Eastern Red Hills (ERH) Centre (Figure 1B and D) [Emeleus and Bell 2005]. The Cuillin Centre is gabbroic, and comprises plutonic bodies, with minor intrusions including arcuate 'cone sheets'. Pegmatitic veins in outer Cuillin gabbro cone sheets have been dated at  $58.91 \pm 0.08$  Ma [Hamilton et al. 1998]. The Western Red Hills Centre typically comprises granitic plutons including the  $58.58 \pm 0.13$  Ma Loch Ainort Granite [Chambers and Pringle 2001]. The Eastern Red Hills Centre typically comprises granitic intrusions, although gabbroic units are also present [Bell 1966; 1976; Emeleus and Bell 2005]. The Eastern Red Hills Centre has been subdivided into two suites: 1) the older Outer Granite comprising granite intrusions forming the hills of Glas Beinn Mhor, Beinn na Cro, Beinn an Dubhaich, and east of Beinn na Caillich to Creag Strollamus, together with the Beinn na Cro and Broadford gabbros and; 2) the younger Inner Granite comprising the granite intrusions forming Beinn na Caillich, Beinn Dearg Mhor, and Beinn Dearg Bheag (Figure 2). The Beinn an Dubhaich Granite has been dated at  $55.89 \pm 0.15$  Ma [M. A. Hamilton, in Emeleus and Bell 2005], whilst a pitchstone dyke cross-cutting the Beinn na Caillich Granite has been dated at  $55.7 \pm 0.1$  Ma [M. A. Hamilton, in Emeleus and Bell 2005] (Figure 2). Emplacement of the Beinn an Dubhaich Granite formed a well-developed contact aureole in the surrounding Cambro-Ordovician country rock [Holness 1992] (Figure 2). To the south east of the Eastern Red Hills Centre, a series of composite intrusions, typically sills with rhyolitic/microgranitic cores and basaltic andesite margins, are emplaced into older country rock.

Large gravity and magnetic anomalies exist over the Cuillin Centre gabbros, and Western and Eastern Red Hills Centre granites, and to the SE of the Eastern Red Hills [Bott and Tuson 1973; Hoersch 1979; Goultly et al. 1996]. These anomalies indicate that gabbro extends below the Cuillin Centre to depths of  $\sim 14$  km [Bott and Tuson 1973]. Above this gabbroic mass the Western and Eastern Red Hills granites were emplaced as shallow sheets at depths to  $\sim 2$  km. The base of these sheets probably consists of interlayered granite and gabbro [Goultly et al. 1996].

The main study area detailed in this paper is  $\sim 7$  km<sup>2</sup> and contains volcanic rocks we term the Kilchrist Volcanic Formation (KVF), which fringe the Beinn na Caillich Granite of

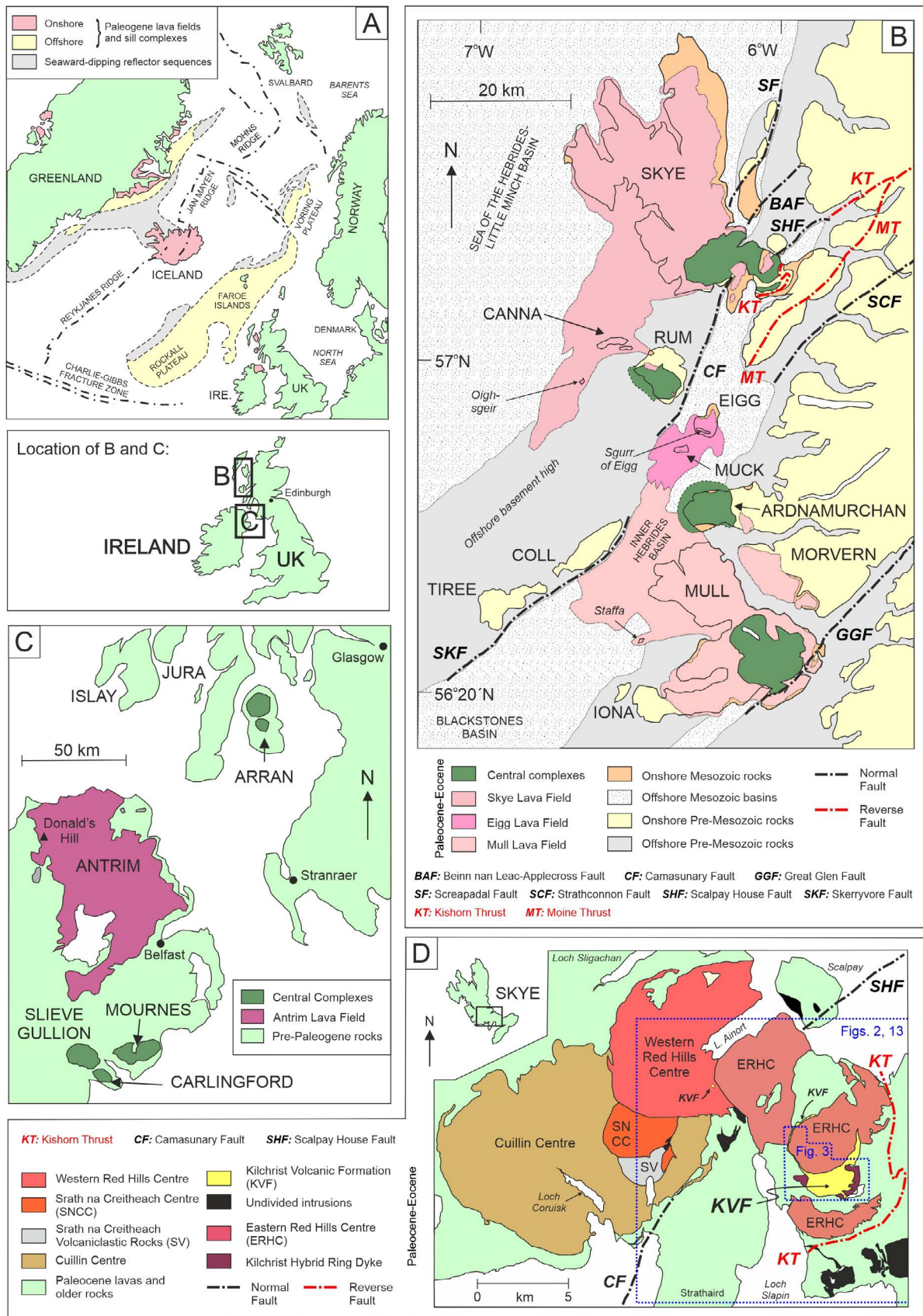


Figure 1: [A] The North Atlantic Igneous Province with [B] and [C] insets showing the British Paleogene Igneous Province (BPIP). [B] The BPIP and relative positions of its lava fields and central complexes (modified from Emeleus and Bell [2005]). Major pre-Paleocene faults are shown in red and black hatched lines. [D] Map of Skye Central Complex showing position of Kilchrist Volcanic Formation (KVF) in relation to gabbroic and granitic intrusions. Locations of Figure 2 and Figure 13 indicated.

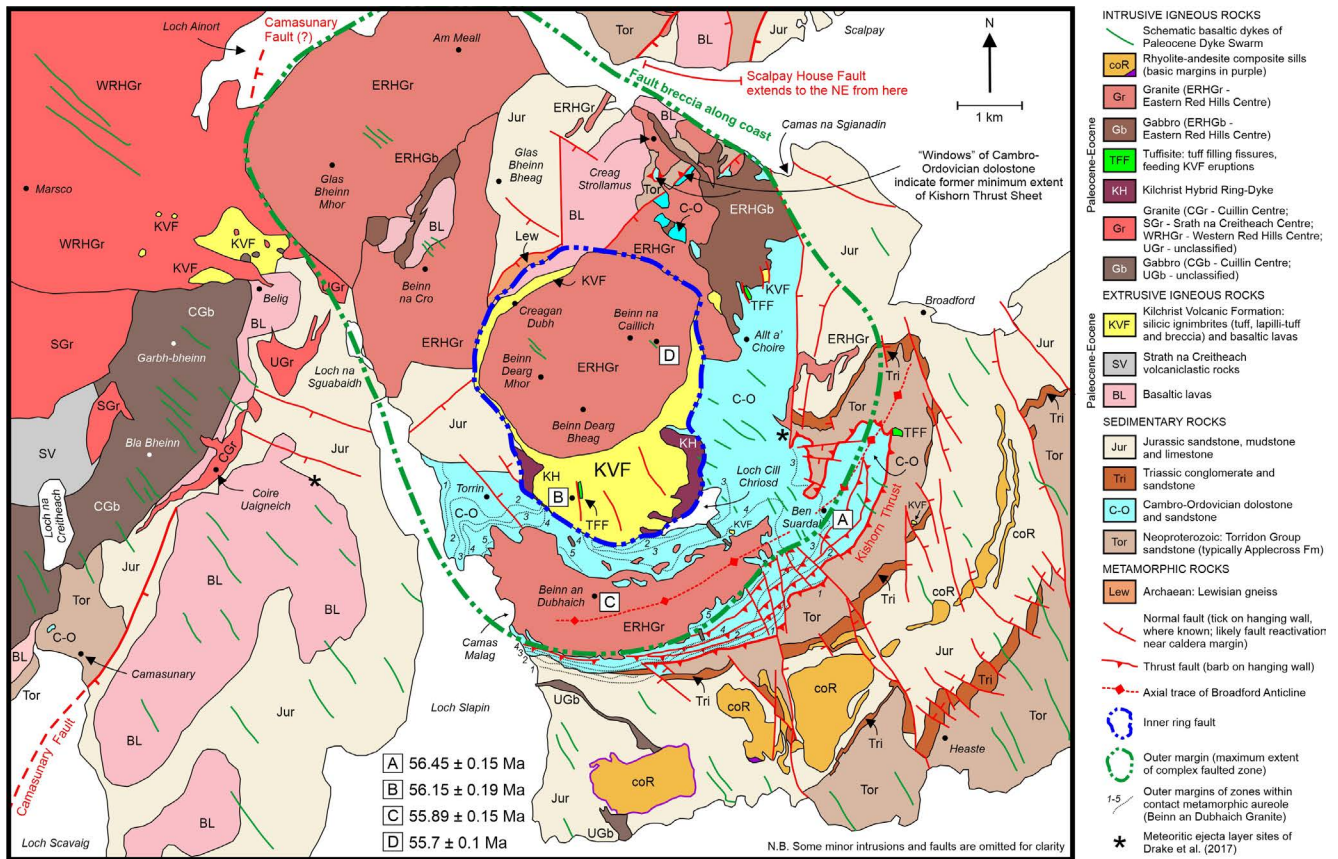


Figure 2: Map of the extent of the Paleocene Kilchrist Caldera, Isle of Skye, NW Scotland (modified from BGS [2005]).

the ERH Centre (Figures 2 and 3). The vast majority of the 600 m-thick KVF is preserved within a semi-arcuate ring structure, partially comprising intrusive igneous rocks. This structure, termed the Kilchrist Hybrid Ring-Dyke, has an external margin which dips steeply outwards ( $\geq 60^\circ$ ) at its eastern extremities, whilst its inner margins dip at  $\leq 15^\circ$  (see Figures 2 and 3) [Bell 1985; Bell and Harris 1986]. The intrusion was first reported as granophyre and linked to cauldron subsidence [Harker and Clough 1904] but has subsequently been reclassified as a hybrid mixed-magma intrusive ('Kilchrist Hybrids') [Bell 1985]. Where the ring-dyke intrusion is not exposed, contacts between country rock and the volcanic rocks are interpreted as part of a ring-fault [Bell 1985; Bell and Harris 1986]. Within this ring-fault/dyke the volcanic pile comprises diverse silicic ignimbrites, fall deposits, and basic lavas. Initially these typically coarse, polyolithic clastic deposits were classified as 'agglomerates' and interpreted as vent-fill material, related to cauldron subsidence [Harker and Clough 1904]. Ray [1962, 1972] identified part of the sequence as 'intrusive ignimbrite breccias'. More detailed work by Bell [1985] identified thin acid and basic tuffs, ignimbrites with fiamme, and acid and basic lavas, including 'hyaloclastite', interbedded with the 'agglomerates' (lapilli-tuffs/breccias). The sequence was interpreted as predominantly extrusive pyroclastic rocks formed at the surface, which underwent subaerial modification/reworking, and preserved in a down-faulted block, rather than in a vent. The tuffs and agglomerates were interpreted

as pyroclastic deposits, and the localised ignimbrites with fiamme related to folding and slumping during rheomorphism. The lavas were interpreted to have erupted during hiatuses in pyroclastic activity, with localised emplacement into water forming hyaloclastite [Bell 1985]. In this study, we re-classify these volcanic rocks as proximal caldera deposits.

We also document extra-caldera ignimbrites belonging to the KVF northwest of the caldera outer margin (Figure 2). Harker and Clough [1904] first suggested that these deposits on Belig formed in a vent that pre-dated both gabbro of the Cuillin Centre, and some granites of the Western Red Hills Centre. Subsequently, Richey [1932] suggested that the Belig deposits were younger than the Cuillin Centre, since they are not cut by cone sheets from this centre. Other workers [Bell 1966; 1976] suggested the Belig deposits represented 'vent filling' intrusive pyroclastic breccia, formed by country rock fracturing, due to gas streaming from underlying silicic magma. In this study we re-interpret the Belig deposits as diverse KVF ignimbrite lithofacies, which post-date the Cuillin and Western Red Hills centres.

### 2.3 Faults and folds on Skye

Numerous faults both pre- and post-date igneous activity and cut the Kilchrist Caldera and the surrounding area. North of the caldera inner ring-fault at Creag Strollamus (Figure 2), part of the NE-SW-trending Moine Thrust Zone crops out, and

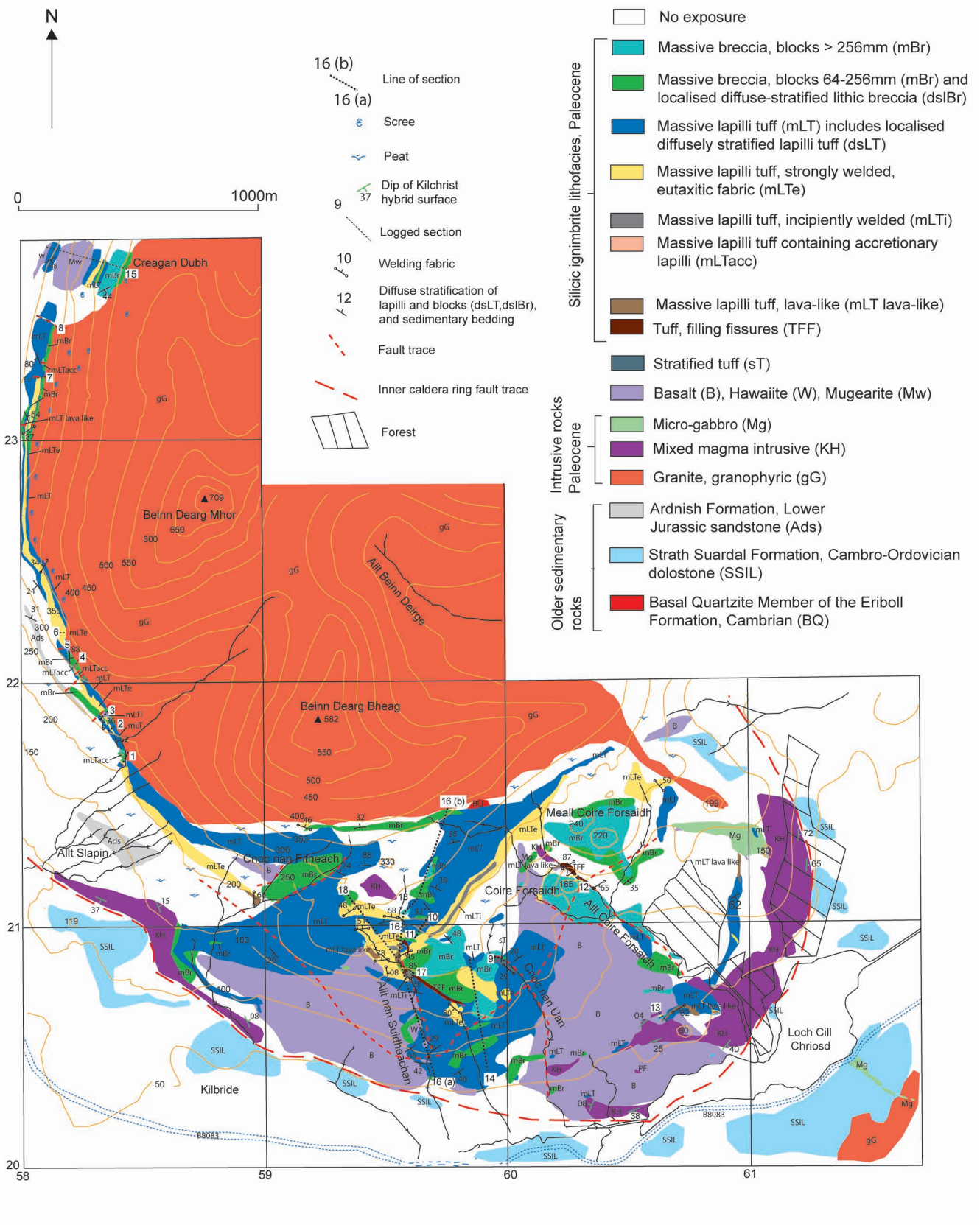


Figure 3: Geological map of the Kilchrist Volcanic Formation (KVF). The numbers round the grid correspond with the British National Grid square (NG). Logged sections 1–18 are detailed in [Supplementary Material 1](#) and correlated in Figures 11 and 12. mBr has been subdivided into blocks 64–256 mm diameter and those >256 mm to highlight the distribution of the coarsest units.

comprises hanging wall Archaean Lewisian gneiss, and Neoproterozoic Torridon Group sandstone (Applecross Formation), together with footwall Ordovician Durness Group dolostone (Strath Suardal Formation). South of Beinn an Dubhaich a ~400 m-wide zone of imbricated Cambro-Ordovician rocks is capped by the southward dipping Kishorn Thrust Fault [Bailey 1955; Barber 1965; Coward and Whalley 1979], where Torridon Group (Applecross Formation) sandstones are thrust over the Cambro-Ordovician dolostone (Figure 2). The thrust fault trace is then postulated to extend SW offshore [BGS 2005]. This imbricated zone caused thickening, tilting, and repetition of footwall lithologies within the Cambro-Ordovician succession.

Skye is situated within two Mesozoic extensional basins which are bounded by NNE/NE–SSW/SW-orientated faults (Figure 1B). North Skye lies within the Sea of the Hebrides Basin which is bounded by the Minch and Camasunary Faults, and South Skye lies within the Inner Hebrides Basin, which is bounded by the Camasunary and Strathconon Faults [Morton 1992; Archer et al. 2019]. Both basins are half grabens, developed on ESE orientated downthrown hanging wall blocks [Butler and Hutton 1994] and both the Cuillin Centre, and eastern margin of the Western Red Hills Centre, are juxtaposed with the Camasunary Fault which bounds both basins. Multi-phase rifting which generated growth of these basins ceased at the end Jurassic in the North Sea [Archer et al. 2019]. The Camasunary Fault partially crops out at Camasunary Bay (Figure 2), but elsewhere on Skye has been largely obscured by Paleocene intrusions. However, the fault trace is considered to be aligned with the NE–SW orientated granite intrusions which crop out in the Coire Uaigneach area [Butler and Hutton 1994]. The trace probably then extends below the westernmost exposures of pyroclastic rocks on Belig [Peach et al. 1910; Bailey 1955; Bell 1966]. To the north and east of the Camasunary Fault are three further Mesozoic extensional faults [Roberts and Holdsworth 1999; Archer et al. 2019] (Figure 1B and D): 1) the Scalpay House Fault; 2) the Beinn nan Leac-Applecross Fault; and 3) the Screapadal Fault (aka Raasay Fault). The Camasunary Fault links kinematically with the Screapadal Fault via a series of NW–SE-trending transfer zones, which have been considered influential in localising granite intrusions on Skye [Butler and Hutton 1994]. The Scalpay House Fault and Beinn nan Leac-Applecross Fault form NE-trending splays to the Camasunary Fault [Archer et al. 2019] and the former is coincident with the Kishorn Thrust trace on the Scottish mainland, and its postulated extent across Skye.

Numerous localised extensional faults are common around the Beinn na Caillich Granite (Figure 2). The faults form a semi-radial pattern and displace Lower and Middle Jurassic aged sedimentary rocks and Palaeocene lavas. Within the Kilchrist Caldera area sporadic NNW–SSE-trending basic dykes of the regional dyke swarm cut sedimentary country rock, ignimbrites of the KVF, and granite of the Eastern Red Hills Centre. In the south of the study area the axial trace of the “Broadford Anticline” [Harker and Clough 1904; Bailey 1955; Nicholson 1985] extends laterally for ~4 km (Figure 2). The structure contains folded Mesozoic and Cambro-Ordovician strata and is considered Paleocene in age [Holroyd 1994].

### 3 METHODS

Mapping and identification of pyroclastic rocks within the study area is challenging. The ignimbrites have been subjected to extensive post-depositional alteration [Drake 2015] and range from low–high in grade [Walker 1983]. Frequently they display complex grading profiles, and interdigitate laterally and vertically with different lithofacies over distances <0.5 m. As such it was frequently necessary to group lithologies together into a dominant lithofacies type for mapping at a scale of 1:10,000. Marker horizons, and way up indicators, particularly in well-exposed stream sections were employed extensively during mapping and logging of pyroclastic sequences. Logs were constructed by using a 75 m length survey tape. Vertical scale log increments therefore do not reflect ordnance datum height data, but rather apparent thickness of units. Apparent thickness of units has been converted to true thickness by use of volcanic fabric within ignimbrites, and other way up indicators wherever possible. Height in relation to logged data therefore refers to cumulative distance in metres and centimetres from the start of the logged section.

U-Pb dating was employed to establish the age of Stage 3 eruptions in the KVF (Figure 17 and Supplementary Material 1). Zircons were isolated using conventional mineral separation techniques, and U/Pb dating of samples was conducted at the NIGL facility, British Geological Survey, Keyworth, Nottingham, UK at the NERC Isotope Geosciences Laboratory. Analysis was performed on a Thermo Triton TIMS. Single analysis U-Pb dates and uncertainties were calculated using the algorithms of Schmitz and Schoene [2007]. Full details of the U-Pb methodology are contained within the Supplementary Material 1. Thin sections were examined using a Zeiss polarising microscope and Electron micro-probe (EMP) analysis on a Jeol JXA8100 Superprobe (WDS), with an Oxford Instruments AZtec system (EDS) at Birkbeck College, University of London. EDS analysis was carried out using an accelerating voltage of 15 kV, current of 1 µA, and a beam diameter of 1 µm with an acquisition time for 20 seconds. A proxy to bulk elemental whole rock analysis was determined by multiple area (100 × 40 µm) scan analysis of representative matrix, carefully avoiding lithic lapilli in the case of ignimbrites, and phenocrysts in the case of lava. Analyses were calibrated against standards of natural silicates, oxides, and Specpure metals with the data corrected using a ZAF program (see Supplementary Material 1 for full EMP methodology).

### 4 LITHOFACIES OF THE KILCHRIST VOLCANIC FORMATION (KVF)

The KVF comprises a complex sequence of lithofacies (Tables 1, 2, 3, 4 and 5, and Figures 4, 5, 6, 7, 8 and 9). In order to determine KVF stratigraphy and volcanic history, 18 logged sections were constructed around the Beinn na Caillich Granite (Figures 2, 11 and 12). The most complete logged section across the study area was obtained from Allt nan Suidheachan and its tributaries (Figure 3 and logs 16, 18 in Supplementary Material 1). Following log correlation four eruption stages were identified in the KVF. The lithofacies de-

tailed below (additional detail given in [Supplementary Material 1](#)) crop out within a caldera inner ring-fault ([Figure 2](#)). KVF lithofacies are also found outside the caldera inner ring-fault but within the caldera outer margin, and also as extra-caldera deposits ([Figure 2](#)). The contact between the Beinn na Caillich Granite and fringing ignimbrites is of an intrusive nature. West of Beinn Dearg Mhor ([Figure 3](#)), ignimbrite juxtaposed with granite is rucked up, whilst at Allt Beinn Dearg (NG 60702 22363) a  $4 \times 2$  m xenolith of ignimbrite is wholly enclosed within the granite. At Kilchrist ignimbrites are bounded within the mixed-magma Kilchrist Hybrid Ring-Dyke to the south ([Figure 3](#)), which marks the inner ring fault of the Kilchrist Caldera. The northern margin of this ring-dyke is absent presumably due to subsequent intrusion of the Beinn na Caillich Granite ([Figures 2 and 3](#)). We also document distinctive and temporally significant silicic inclusions in basic intrusions fringing the caldera ([Figure 10](#)).

#### 4.1 KVF lithofacies outside the inner ring-fault, and within the outer margin

Widely dispersed, sporadic, small ( $\leq 5 \times 5$  m) exposures of mLT<sub>e</sub> and mLT lava-like are evident outside of the caldera inner ring-fault to the north east, south and east ([Figure 2](#), [Figure S10A–D](#)). Rhyolitic tuff crops out within a NW-trending linear fissure in Allt a Choire (Corrie Rd) east of the inner ring-fault ([Figure S10B–D](#)). The tuff is ~1 m thick and has a pronounced linear fabric comprising alternating planar bands and spherulites ([Figure S10C](#)). Groundmass EMP scans plot in the rhyolite field on a T.A.S. diagram ([Figure S13](#); [Supplementary Material 1](#)). mLT lava-like crops out in close proximity to the Allt a Choire tuff as an isolated exposure surrounded by Cambro-Ordovician dolostone ([Figure S10D](#)). The unit is <1 m thick, fractured, cut by cooling joints, and has an intense planar fabric which pervades the rock. Mafic enclaves with lobate margins are evident on weathered surfaces as rust-coloured blotches. Chemically this mLT lava-like plots within the same TAS diagram field as the fissure fed tuff within the Allt a Choire stream section. Other silicic ignimbrite localities are evident within the caldera outer margin. Approximately 1 km SE of Loch Cill Chroisd highly chloritised mLT lava-like, crops out in a 4 m linear depression orientated  $060^\circ$  ([Figure 2](#)).

#### 4.2 Extra-caldera KVF lithofacies

We have identified diverse KVF ignimbrite lithofacies (mLT, mBr, mLT<sub>acc</sub>, sT) outside of the NW caldera outer margin on Belig ([Figures 2 and 9](#)). A variety of lapilli and block types are present in these units, including granitic clasts ([Figure 9B](#)) that cannot be provenanced to the local area [[Bell 1966](#)]. The matrix is comminuted, partially chloritised, and quartz crystals are frequently mechanically fractured. The lowermost Belig ignimbrites typically comprise both normal and reverse graded rhyolitic mLT and normally graded mBr (NG 54301 25012) ([Figure 9A, B](#)). Above these units stratified tuff (sT) (NG 54301 24908) is present containing post-depositional chloritised concretions which overgrow fabric without displacing it ([Figure 9C](#)) and comprises alternating leucocratic domains of quartz and feldspar, together with melanocratic domains of opaques, and unresolved mafic lithic lapilli/enclaves. In close

proximity, accretionary lapilli are contained within a 20 m-thick mLT<sub>acc</sub> unit ([Figure 9D](#), NG 54325 24866). This unit has a pronounced fabric, and contains rounded to subrounded lithic lapilli in the size range 0.7 mm–1.6 cm. This unit is chemically and visually very similar to KVF mLT<sub>acc</sub> within the caldera ([Figure 5](#) and [Supplementary Material 1](#), logs 1, 4, and 5). The mLT<sub>acc</sub> unit on Belig is preceded by mBr, and succeeded by massive lapilli tuff (mLT) and diffuse stratified lapilli tuff (dsLT). This is the same volcanic stratigraphy seen within some units at Kilchrist ([Figure 5C](#), and [Supplementary Material 1](#), log 4). Above the mLT<sub>acc</sub>-dsLT unit, we identified three repeating mLT-mBr sequences ([Figure 9F, G](#)) on a traverse of the northern spine of Belig between NG 54325 24866 and 54345 24591. The largest block size noted on this traverse was  $90 \times 70$  cm. Within some mBr there is evidence of partial melting of incorporated blocks (NG 54346 24860). At this locality oversized gabbroic blocks ( $\leq 70 \times 60$  cm) have lobate margins, which chill into an external fabric within matrix-to clast-supported mBr ([Figure 9G](#)). Such repeating mLT-mBr cycles, and similarity in maximum block size accords well with some KVF eruptive units at Kilchrist (logs 1, 6, 8, 10, and 15). Belig and the Kilchrist study area are the only Skye localities known to the authors where repeating sequences of mLT and mBr crop out within ignimbrites. The Belig deposits, first detailed by [Bell \[1966, 1976\]](#) were previously classified as intrusive pyroclastic breccia. We reinterpret them as deposits of PDCs that waxed and waned, spatially and temporally, during the later stages of the eruptions at Kilchrist which produced the KVF. Individual ignimbrite units could have been considerably thicker upon deposition, but were subsequently eroded by later, coarser, progressively aggrading ignimbrites.

#### 4.3 Silicic inclusions in basic intrusions

Silicic inclusions are found within a basic dyke cutting Cambro-Ordovician dolostone near the SE caldera outer margin on the eastern summit side of Ben Suardal. The dyke is ~300 m long, 5 m wide ([Figure 10A, B](#)), orientated on a non-regional swarm trend ( $220^\circ$ ), has pronounced feathered chilled margins, and contains multiple rounded granitic inclusions ranging from 8–17 cm in diameter. Numerous inclusions have exfoliated outer rims and are often clustered in small groups ([Figure 10B](#)), and some inclusions exhibit lobate margins. The inclusions comprise quartz, albite and K-feldspar as major phases together with minor titanite, allanite and zircon. The typically rounded/lobate nature of the inclusions indicates that they may be partially melted xenoliths, or contemporaneous magmatic enclaves. These inclusions visually, mineralogically, and chemically resemble granitic lapilli found in the deposits at Belig ([Figure 9B](#)).

## 5 EVIDENCE FOR THE KILCHRIST CALDERA

### 5.1 Inner ring-fault

We interpret the southern margin of the inner ring-fault as being delineated by the Kilchrist Hybrid Ring Dyke ([Figure 2](#)). Two isolated exposures of hybrid intrusive also crop out interior to the ring dyke/ring-fault structure ([Figure 3](#)). The pres-

Table 1: Basic lavas, paleosols, ash horizons, and peperite of the KVF.

Rock name	Spatial distribution	Field characteristics	Thin section characteristics	Interpretation
Basic lavas: (Tholeiite, Hawaiiite, Mugearite)	Lava stratigraphy is best observed in Allt nan Suidheachan (log 16: <a href="#">Supplementary Material 1</a> ), where 4 flows have total thickness of ~8 m. Each flow is capped by either a paleosol, or tuff layer ( <a href="#">Figure 4A, B</a> ). Around Creagan Dubh both hawaiiites (log 15: <a href="#">Supplementary Material 1</a> ), and mugearites (log 15: <a href="#">Supplementary Material 1</a> ) form prominent crags ( <a href="#">Figure S1A</a> ).	Tholeiitic basalts dominant with highly subordinate hawaiiites and mugearites. Chemically, tholeiites are akin to the Skye Main Lava Series [ <a href="#">Bell 1984</a> ]. Zeolites occur at top of flows. The majority are oblate ( <a href="#">Figure 4B</a> ), whilst less rounded, towards flow bases. Mugearite is aphanitic, blocky, and cut by irregular joints.	Tholeiitic olivine basalt contains augite and forsterite ( <a href="#">Figure 4C</a> ), turbid Ca-rich feldspars, and chloritised CPX with calcite reaction rims. Hawaiiite lacks amygdales, possesses abundant olivine (Fo78-55), labradorite (An55-61), and chloritized CPX. Mugearite contains andesine-labradorite (An30-55), and typically has a flow aligned groundmass.	Lavas were fissure fed via regional dyke swarm. Tholeiites generated from partial melting of depleted mantle source, and contemporaneous contamination [ <a href="#">Bell and Williamson 1994</a> ]. Further fractionation produced hawaiiites and mugearites [ <a href="#">Thompson et al. 1982</a> ].
Paleosols, ash horizons and peperite	Within Allt nan Suidheachan (log 16: <a href="#">Supplementary Material 1</a> 290–296 m) ( <a href="#">Figure 4A, B</a> ).	Two $\leq 5$ cm-thick, dark red, fine grained paleosols (fade in colour towards underlying tholeiite) and 4 cm-thick red laminated ash horizons (sharp contact with tholeiite) are intercalated between tholeiite lava flows in Allt nan Suidheachan ( <a href="#">Figure 4A, B</a> and log 16: <a href="#">Supplementary Material 1</a> ). Rare localised, normally graded peperite is present as a $\leq 20$ cm-thick layer at the base of the uppermost tholeiitic lava in Allt nan Suidheachan (log 16: <a href="#">Supplementary Material 1</a> ).	Paleosols contain K-feldspar, quartz, plagioclase, albite, magnetite. Ash horizons contain augite, quartz, plagioclase, lithic fragments and bubble wall margins ( <a href="#">Figure 4D</a> ). Groundmass phases include K-feldspar, zircon, and chrome spinel with magnetite rims. Peperites comprise lobate mafic clots $\leq 4$ cm in length, surrounded by highly friable ash to granular matrix. Clots are either completely isolated or clustered in a jigsaw fit, separated by matrix.	Paleosols indicate hiatuses of 100s–1000s of years between flows [ <a href="#">Retallack 1988</a> ]. Ash horizons fell during eruptions with ash accumulating on top of lava flows. Peperite indicates paleosurfaces were locally covered with unconsolidated wet sediment, and interacted with lava [ <a href="#">White et al. 2000</a> ]. Normal grading results from initial settling of larger mafic clasts during peperite formation [ <a href="#">Brown and Bell 2007</a> ].



Table 2: Stratified tuff (sT) and accretionary lapilli-bearing massive lapilli tuff (mLTacc) of the KVF.

Rock name	Spatial distribution	Field characteristics	Thin section characteristics	Interpretation
Stratified tuff (sT)	(sT) is rare and only found in Cnoc Nan Uan (Figures 3, 5 and 12, log 9: <a href="#">Supplementary Material 1</a> ) and on Belig (Figure 9).	Kilchrist unit is ~3.5 m-thick, columnar jointed (Figure 5A, Figure S2B), and laterally extensive for ~20 m. It is juxtaposed with mBr and mLT. Unit comprises alternating fine grained, melanocratic and leucocratic laminations $\leq 1$ mm-thick (Figure S5A). Matrix content $\geq 95\%$ , with sporadic arkosic sandstone lithic fragments frequently ash draped (Figure 5B).	Rhyolitic matrix comprising quartz, K-feldspar, albite, titanite, chlorite, allenite, and zircon. Leucocratic laminations comprise normally graded domains (Figure 5B) which alternate with thinner ungraded melanocratic domains. Microscale cross-stratification) evident together with loading, syn-sedimentary faulting, and normal grading of ash grading (Figure 5B).	Deposition was via direct fall-out from eruption clouds (evidenced by ash drapes and laminations). Ash was necessarily hot due to the presence of contractional cooling joints. Loading and cross stratification indicates subaqueous reworking took place following deposition. Brittle offset of layers was probably induced by volcano-tectonic faulting.
Accretionary lapilli bearing mLT (mLTacc)	Ash aggregate-bearing units fringe the Eastern Red Hills Centre laterally over 1.5 km (Figures 3 and 5C, D, logs 1, 4, 6, 8 <a href="#">Supplementary Material 1</a> ) and on Belig (Figures 2 and 9D)	Two units 80 cm and 3 m-thick, contain acc lithic lapilli (Figure S2E, F, H), and sporadic cored acc lithic lapilli crop out on Belig (Figure 9C). Both units have a fine-grained, crystal-poor, vitroclastic matrix ( $\geq 90\%$ ), containing linear trails of normally graded (Figure 9E, F), spherical to subspherical cored and oblate acc lithic lapilli (Figure S2F, H).	Chemically mLTacc matrix varies from basaltic andesite to dacite ( <a href="#">Supplementary Material 1</a> , Figure S13), fine-grained, contains broken glass shards, and small basaltic and granitic lapilli fragments ( $\leq 50\text{--}130\ \mu\text{m}$ ). Matrix phases comprise K-feldspar, quartz, clinopyroxene, Ca-plagioclase, oligoclase, zircon, chrome, spinel, rutile, epidote and biotite.	Ash pellet grew into accretionary lapilli by coalescence of wet ash within turbulent up drafted plumes [ <a href="#">Van Eaton et al. 2015</a> ]. Growing lapilli reached a critical density and fell into underlying PDCs and grew [ <a href="#">Brown et al. 2010</a> ]. The presence of oblate accretionary lapilli (Figure S2H) indicates that PDCs were moist enough to promote syn-post depositional soft-state deformation.

Table 3: Massive breccia (mBr), diffuse stratified lithic breccia (dslBr), massive lapilli tuff (mLT), and diffuse stratified lapilli tuff (dsLT) of the KVF.

Rock name	Spatial distribution	Field characteristics	Thin section characteristics	Interpretation
Massive breccia (mBr) and diffuse-stratified lithic breccia (dslBr)	mBr forms crags south of Beinn Dearg Bheag, west of Cnoc Nam Forsaidh, and Meall Coire Forsaidh. dslBr crops out localised around the upper reaches of log 16 (Figure 3 at NG 59488 21333).	Variably matrix to clast supported, and small blocks (64–256 mm) to large blocks (>256 mm). Compositionally blocks are subangular–subrounded, heterolithic (arkosic sandstone, amygdaloidal and aphanitic basalt, quartzite, calcareous sandstone, dolostone, mLTi, mLTe, mLT lava-like and mBr; Figure 6A, B). May be ungraded, graded or reverse graded. Exfoliation and thermal spalling of rounded blocks (Figure S3B and log 16, 50 m: Supplementary Material 1) is a common feature of reverse graded mBr. dslBr has bi-modal block population (i.e. mBr and mLTi are >56 mm, and basalt blocks are smaller).	mBr matrix is typically dacite-rhyolitic (Figure S12: Supplementary Material 1) and contains chloritised former bubble wall shards, subrounded quartz crystals, K-feldspar, albite, chlorite, zircon, epidote, titanite, sporadic allanite, pyrite and calcite. Mechanical fracture of incorporated blocks is common at both macro-scale and in thin section (Figure S3A). Aphanitic type II mafic enclaves [Troll et al. 2004] are strongly deformed around matrix lithic fragments. Matrix supported mBr may contain sporadic gas-escape structures including lithophysae (log 15, Supplementary Material 1).	Deposition of mBr and dslBr took place at flow boundaries dominated by fluid-escape processes [Branney and Kokelaar 2002]. Heat-derived features within mBr indicate genesis within ‘hot’ high particle concentration PDCs. Grading reflects periodic current unsteadiness. The presence of mafic enclaves indicate basic melt was periodically incorporated into PDCs [Sparks et al. 1977; Eichelberger 1980; Folch and Martí 1998]. Diffuse stratification within dslBr was promoted by turbulence.
Massive lapilli tuff (mLT) and diffuse-stratified lapilli tuff (dsLT)	mLT is the most abundant type of ignimbrite (Figure 3) throughout the study area, cropping out as ≤10 m-thick, laterally impersistent units, which frequently interdigitate with other ignimbrite lithofacies. Diffuse stratified lapilli tuff (dsLT) crops out sporadically throughout the extent of the southern inner ring-fault (Figure 2).	Variably matrix to clast supported, mLT lapilli populations are heterolithic with ungraded mLT (Figure 6A), being most common, followed by reverse graded, and highly subordinate normally graded mLT. Lapilli are highly angular–subangular, and the dominant types are arkosic sandstone and quartzite. Subordinate types are amygdaloidal basalt, dolostone, mLT, mLTe, mLT lava-like, and mBr. Heat features such as lithophysae, contractional cooling joints, and thermal spalling are common features within mLT. dsLT units may be reverse to normally graded (Figure S4A), with matrix coarse ash-granule grade (Figure 6B).	Matrix variably basaltic-basaltic andesite-rhyolitic-trachytic (Supplementary Material 1, Figure S12) and vitric to medium grained. Ubiquitous subrounded quartz crystals ≤2 mm diameter (Figure S5A), type II and III mafic enclaves (Figure 6E), alkali feldspars with fritted margins (Figure S4C), fan spherulites (Figure S5B) and resorbed quartz crystals (Figure 6C) are common within matrix. Matrix lithic fragments (60–250 μm) are granitic to basaltic in affinity. Undeformed glass shards within lapilli pressure shadows are common. Former glass is frequently devitrified, and amorphous (Figure 6C). Calcite is often present as late-stage cross cutting vein infill.	Deposition of mLT took place within high-concentration, fluid-escape dominated, depositional flow boundary zones [Branney and Kokelaar 2002]. Conditions within PDCs fluctuated throughout eruptions (evidenced by grading of lapilli). Reverse grading of lithic lapilli reflect increases in conduit flux during sustained eruptions. Diffuse stratification indicates subtle unsteadiness within the flow-boundary zone attributed to successive surges in fluctuating sustained currents, frictional effects within granular flow-dominated flow boundary zones, or, periodic turbulent eddies [Branney and Kokelaar 2002].

Table 4: Incipiently welded massive lapilli tuff (mLTi) and massive lapilli tuff with eutaxitic fabric (mLTe) of the KVF.

Rock name	Spatial distribution	Field characteristics	Thin section characteristics	Interpretation
Massive lapilli tuff, incipiently welded (mLTi)	mLTi crops out south and west of the Eastern Red Hills Centre laterally over ~400 m south of Beinn Dearg Bheag (Figure 3, log 10, 16–18: <a href="#">Supplementary Material 1</a> ), and over ~1 km west of Beinn Dearg Mhor (Figure 3, log 1 and 15: <a href="#">Supplementary Material 1</a> ).	mLTi units (Figure 7E) laterally discontinuous over distances of $\leq 5$ m grading into mLT, mBr, mLTe, or mLT lava-like. mLTi units frequently contain cooling joints (Figure 7F, Figure S6C, G). Lapilli may comprise subangular–subrounded basalt, quartzite, arkose, or mLTe. Fiamme ( $\leq 15$ cm in length) are common in matrix (Figure S6G) frequently have swallow tails (Figure 7H).	Groundmass is rhyolitic containing angular quartz lapilli (Figure S12), silicate melt globules (Figure S6B), allanite, pyrite, polycrase, xenotime, zircon, deformed bubble wall shards, and resorbed mechanically fractured quartz. Incipient welding of matrix fabric glass shards ( $\leq 2$ $\mu\text{m}$ across) deflected around lithic lapilli (Figure 7G, H). Type III mafic enclaves are common within the matrix.	Deposition took place within high-concentration, fluid-escape dominated, depositional flow boundary zones of ‘hot’ PDCs [ <a href="#">Branney and Kokelaar 2002</a> ]. Reverse grading of mLTi units (logs 17, 18 <a href="#">Supplementary Material 1</a> ) suggests flux levels increased towards the latter stages of mLTi producing eruptions. Within these units, reverse grading of mafic blebs also suggests increased tapping of subsurface mafic melt.
Massive lapilli tuff with eutaxitic fabric (mLTe)	mLTe with pronounced eutaxitic fabric crops out to the south and west of Beinn Dearg Bheag (Figure 3, logs 10,13,14,16,17,18 <a href="#">Supplementary Material 1</a> ) and west of Beinn Dearg Mhor (Figure 3, logs 1,2,6,7,15 <a href="#">Supplementary Material 1</a> ).	Individual mLTe units may range from 1–40 m in thickness, but vast majority are $< 4$ m thick. Weathered surfaces are frequently white (Figure 7A), whilst fresh rock is commonly black or dark grey. Cooling joints are common. Matrix is $\leq 90$ %. Fine grained -glassy, Matrix welding states may be highly variable over $< 0.5$ m. Lithic lapilli comprise amygdaloidal basalt, aphanitic basalt, mLT, mLTe, mLT lava-like, arkosic sandstone, or quartzite and may show evidence of rotation during transportation.	Matrix is rhyolitic (Figure S12: <a href="#">Supplementary Material 1</a> ), fine grained with mechanically fractured quartz $> 55$ % alkali feldspar, chlorite, accessory allanite and zircon, embayed quartz and type II and III mafic enclaves (Figure S7G, H) are common. Eutaxitic matrix fabric (Figure 7B) is deformed around lithics (Figure S7F–H). Matrix lithics are subangular to subrounded, and comprises granite, aphanitic basalt, amygdaloidal basalt, and arkosic sandstone. Un-deformed glass shards are within pressure shadows adjacent to lithic lapilli.	Deposition of mLTe units took place within high-concentration, fluid-escape dominated, depositional flow boundary zones of ‘hot’ PDCs likely to have been $> 600$ °C, because welding of rhyolite commences above this temperature [ <a href="#">Bierwith 1982</a> ]. PDCs were generated from low-fountaining fissure events. Type II and type III mafic enclaves within the matrix, indicate mafic melt was introduced into rhyolitic PDCs throughout eruptions.

Table 5: Lava-like ignimbrite (mLT lava-like), and Tuff filling fissures (TFF) of the KVF.

Rock name	Spatial distribution	Field characteristics	Thin section characteristics	Interpretation
Lava-like ignimbrite (mLT lava-like)	mLT lava-like ignimbrites crop out west of Beinn Dearg Mhor (Figure 3, log 7: Supplementary Material 1) and south of Beinn Dearg Bheag (Figure 3, and log 12, 13, and 16 Supplementary Material 1).	In hand specimen mLT lava-like is flow banded, vitrophyric, and contains $\leq 5\%$ angular lithic lapilli $\leq 30$ mm diameter. Frequently weathered rind pervades $\leq 2$ mm (Figure S8A, B). Banding is on a sub-mm scale, and often forms recumbent folds (Figure S8A), antiform-synform pairs, or ptygmatic folds. An intense fabric is frequently deflected around lithic lapilli (Figure S8B), and amorphous, type II enclaves (Figure 8C).	Fine grained rhyolitic, highly matrix-rich ( $\leq 95\%$ ), (Figure S12: Supplementary Material 1). Main matrix phases are quartz, alkali feldspars, and highly subordinate plagioclase, rutile, chlorite, zircon and monazite. A sublinear parataxitic fabric pervades matrix, which comprises alternating leucocratic $\mu\text{m}$ -thick laminations (quartz, alkali feldspar and rare monazite) and melanocratic (highly chloritised, allenite, titanite) fan spherulites (Figure S9A) laminations. Lapilli of micro-granite, rhyolite, and basalt. Matrix fabric deformed around type II and III mafic enclaves (Figure 8C).	Deposition of mLT lava-like units took place incrementally during very hot ( $\leq 1000$ °C) sustained eruptions, from low, fissure fed fountaining columns [Branney and Kokelaar 1992; 2002]. Macroscale evidence of extremely 'hot' $\sim 1100$ °C [Andrews and Branney 2011] emplacement evidenced by flow banded vitrophyric texture, spherulitic domains, and lithophysae. Ubiquitous matrix mafic blebs indicates extensive magma-mingling between rhyolitic, and mafic-rich melt bodies, throughout mLT lava-like producing eruptions.
Tuff filling fissures (TFF)	Fissure filled tuff $\pm$ brecciated tuff crops out along NW–NNW-trending linear outcrops in the south of the study area (Figure 3, and logs 11,12,17 Supplementary Material 1). The most extensive fissure is 380 m long and broadly parallels the east bank of Allt nan Suidheachan (Figure 3).	Tuff contains sporadic mafic lithic fragments ( $\leq 4$ mm diameter) and ubiquitous chloritised type III enclaves. Lithophysae and sheath folds are common throughout. Intense 'rheomorphic' matrix folding occurs around pumiceous fragments. Fissure thickness range from 5 cm–20 m. Tuff commonly weathers white (Figure 8E, F), has an intense near vertically orientated fabric, and contains sheath folds whose axes are subparallel to the pervasive vertical fabric (Figure 8F). In hand specimen tuff contains sporadic angular mafic lithic fragments and ubiquitous type III enclaves $\leq 1$ cm diameter. Fissures frequently coincide in orientation with NNW-trending dykes of the regional Paleogene swarm	Tuff is rhyolitic (Figure S13: Supplementary Material 1). Thin sections comprise $\leq 95\%$ devitrified glass and abundant spherical spherules (0.5–4mm, diameter) of radiating crystals of quartz and alkali feldspar. Tuff matrix frequently pervaded by perlitic cracks, and contains type II and III mafic enclaves, together with dendritic alkali feldspar crystallites, and rare magnetite and pyrite. There is extremely similar matrix chemistry to very close proximity mLT lava-like, mLT <sub>e</sub> , and fissure fed tuffs.	TFF was generated within fissures as silicic magma expanded and degassed during ascent and was then erupted from upwards flaring fissures. The extremely close proximity of mLT lava-like and mLT <sub>e</sub> to fissure fed tuffs, together with similar matrix chemistry suggests high grade ignimbrites were fissure fed during very 'hot' eruptions. The presence of mafic enclaves within all fissure fed tuff suggests basic magma pulses were incorporated into silicic chambers throughout fissure fed eruptions. Sporadic fissures were 're-exploited' by later NNW-trending basic dykes of the regional swarm since they chill into, and are juxtaposed with, fissure fed tuff (Figure S10E, log 11: Supplementary Material 1).

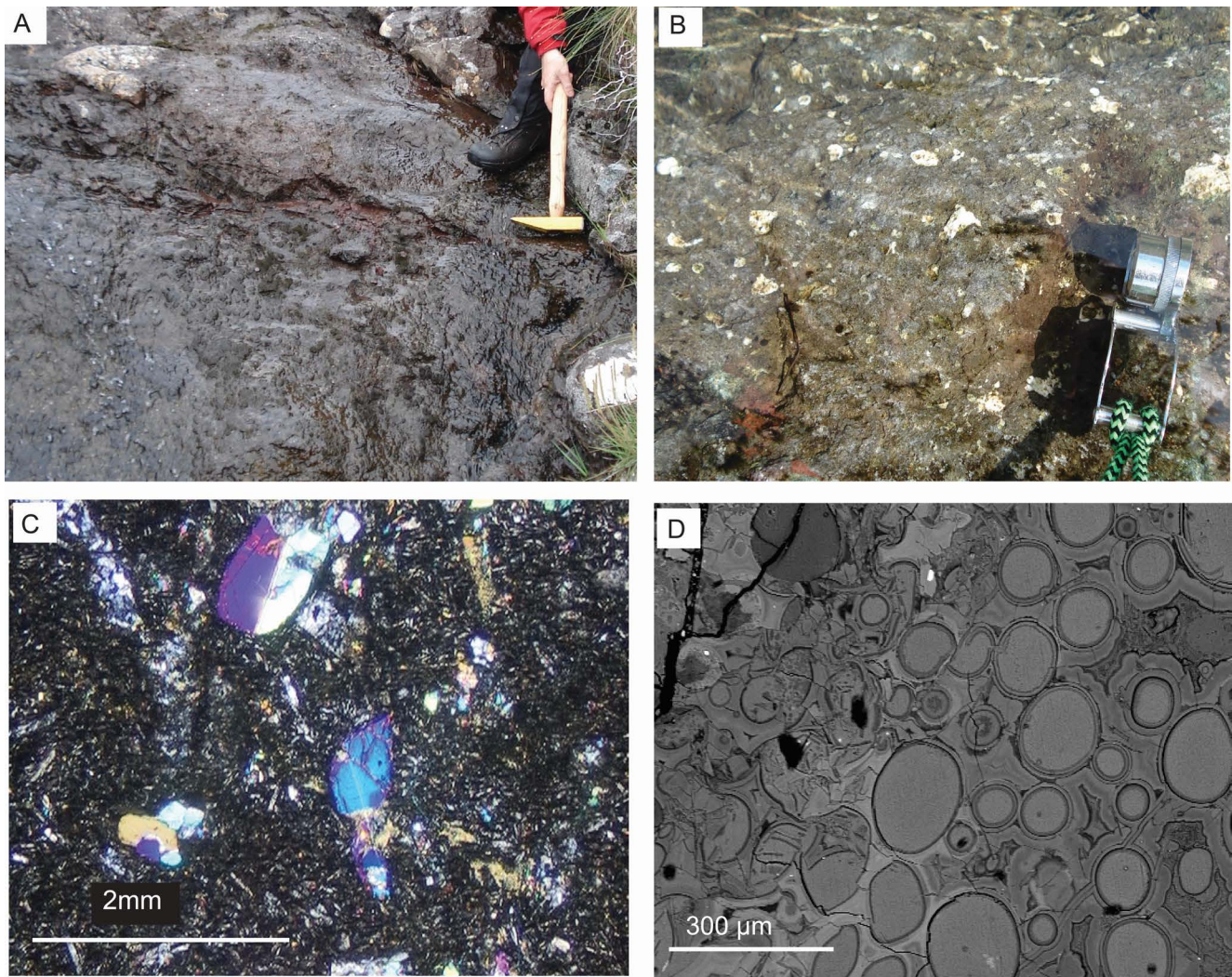


Figure 4: [A] 5.5 cm-thick dark red, fissile paleosol grading into underlying amygdaloidal basalt within Allt Nan Suidheachan, (log 16, 290m height, see [Supplementary Material 1](#)). [B] Amygdaloidal basalt above paleosol in [A]. Reddening in lower left is the colour of the laterally discontinuous paleosol. [C] Tholeiitic basalt containing zoned, twinned forsterite and randomly orientated bytownite groundmass laths, XP, field of view 2 mm (log 16, 355 m height, see [Supplementary Material 1](#)). [EMP backscatter image of bubble wall shards and axiolitic devitrification of bubble wall margins within fall deposit in Allt nan Suidheachan (log 16, 295 m height, see [Supplementary Material 1](#)).

ence of dolostone juxtaposed with, at the same topographic level as, and dipping away from the outer margin of the ring-dyke (Figure 3) suggests that the intrusion displaced Cambro-Ordovician dolostone country rock [Bell 1985; Bell and Harris 1986] and that subsidence of pyroclastic rock took place during caldera down-faulting. Such evidence, together with the presence of ring-dykes and ring-faults, has previously been cited as criteria for identification of BPIP calderas [Brown et al. 2009]. The presence of a possible second arcuate ring-fault between 140–150 m OD (Figure 3) also may provide further evidence of caldera collapse, although the variable dips in volcanic fabric that define this structure could represent downsag of the volcanic fill across faults [Cole et al. 2005].

Different ignimbrite lithofacies are frequently juxtaposed cropping out on opposite stream banks and at waterfalls throughout the study area (Figure 3, [Supplementary Material 1](#), logs 1, 9, 12, 16, and 18). Such exposures often ex-

tend for several hundred metres along stream sections. In Allt nan Suidhachan, fault gouge is sandwiched between mBr and near horizontally orientated columnar cooling joints of mLTi (Figure 6D). Within the inner ring-fault the orientation of fault traces are approximately radial and cofoci with the Beinn na Caillich Granite (Figure 2). We interpret such fault traces as ‘volcano-tectonic faults’, typical of collapse calderas, where displacement was intimately associated with subsurface magma movement and/or eruption [Branney and Kokejar 1994]. We note many fault traces within the study area have trends consistent with the regional NW–NNW North Atlantic extensional trend. Faulting therefore cannot necessarily be solely attributed to volcano-tectonic causes.

Our calculations for the KVF thickness (Figure 3, line of section A–B = ~600m) greatly exceed previous research which suggested ‘chaotic, polyolithic agglomerates’ in the study area (re-classified in this paper as mLT and mBr) were  $\geq 300$  m

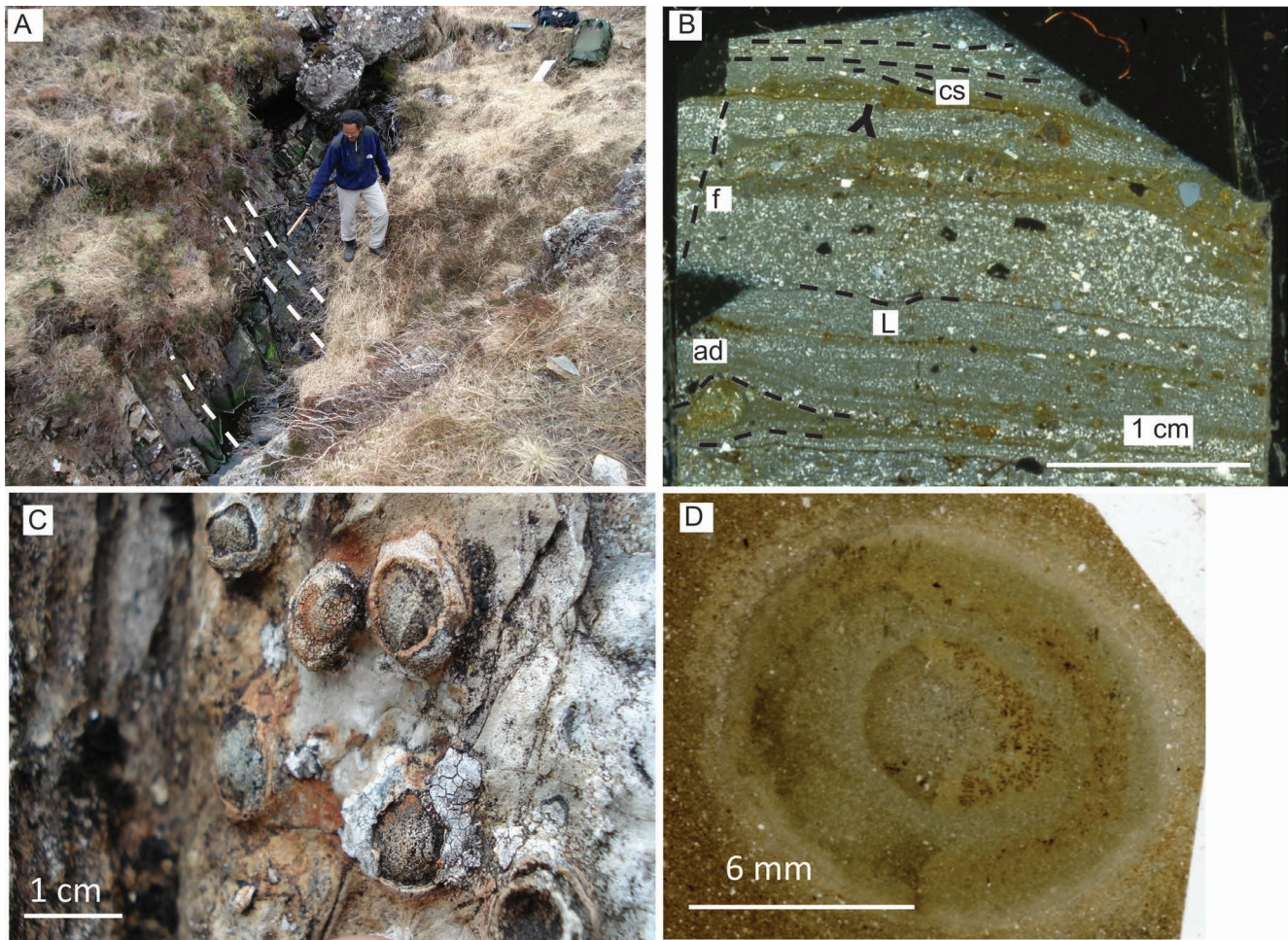


Figure 5: Field and petrographic characteristics of stratified tuff (sT) and accretionary lapilli bearing massive lapilli tuff (mLTacc). [A] Columnar cooling joints within sT on the west bank of Cnoc nan Uan (log 9, 3 m height, see [Supplementary Material 1](#)). Columns are juxtaposed with mLT on east bank and highlight a faulted contact running down the stream. [B] Scan of sT from Cnoc nan Uan in XP, loading structures (L), cross stratification (cs), ash drapes (ad). Offset of layers as a result of faulting (f). [C] Cored accretionary lapilli in mLTacc in discontinuous sublinear trails (log 4, 21 m height, see [Supplementary Material 1](#)). [D] Scan of accretionary lapilli in mLTacc showing normal grading from core to rim and fine grained nature of silicic matrix.

thick [Bell 1985]. Within Stage 4 eruptions (see below) we note the thickness of mBr sequences changes abruptly across volcano-tectonic-induced fault traces in the northeast of the study area. At Meall Coire Forsaidh (Figure 3) a 65 m-thick mBr crops out north-east of a substantial fault trace in Allt Coire Forsaidh (log 12: [Supplementary Material 1](#)). Two hundred metres south-west of this stream, a 30 m-high crag of massive breccia crops out at Coire Forsaidh. Substantial thickness changes in both Stage 4 mBr and mLT (Figure 3) also crop out across fault traces further west at Cnoc nan Uan, Cnoc nan Fitheath and Allt Slapin (Figure 3). Thick sequences of alternating lapilli- and block-rich ignimbrites (mLT and mBr respectively) are a common characteristic of both recent (273 ka Las Canadas, Tenerife [Smith and Kokelaar 2013]) and ancient (460–470 Ma, Scafell Caldera, English Lake District [Branney and Kokelaar 1994]) caldera settings. Such alternating sequences of mLT and mBr are common within Stage 1 and 4 KVF (Figures 11 and 12, and [Supplementary Material](#)

1). Paleo-caldera floors which subside in a complex multi-block faulted (piecemeal) manner [Cole et al. 2005], may be indicated by thickness changes in successive ignimbrites, within the same eruptive episode [Branney and Kokelaar 1994]. The field evidence suggests that such complex faulting took place throughout KVF eruptions.

## 5.2 Outer margin/Extra-caldera

We have interpreted the caldera outer margin as the limit of a complex zone containing numerous faults and a variety of resurgent intrusions. The caldera's northwest outer margin (Figure 2) is delineated by an intrusive contact between the Western and younger Eastern Red Hills granites (Figures 1 and 2). This contact is partially aligned with the postulated on-shore trace of the Camasunary Fault. In the NE of the caldera, from Ob Apoldoire to Camus na Sgianadin (Figure 2), brecciated blocks of Neoproterozoic Torridon Group sandstone and Palaeocene hornfelsed basalt crop out. These blocks are

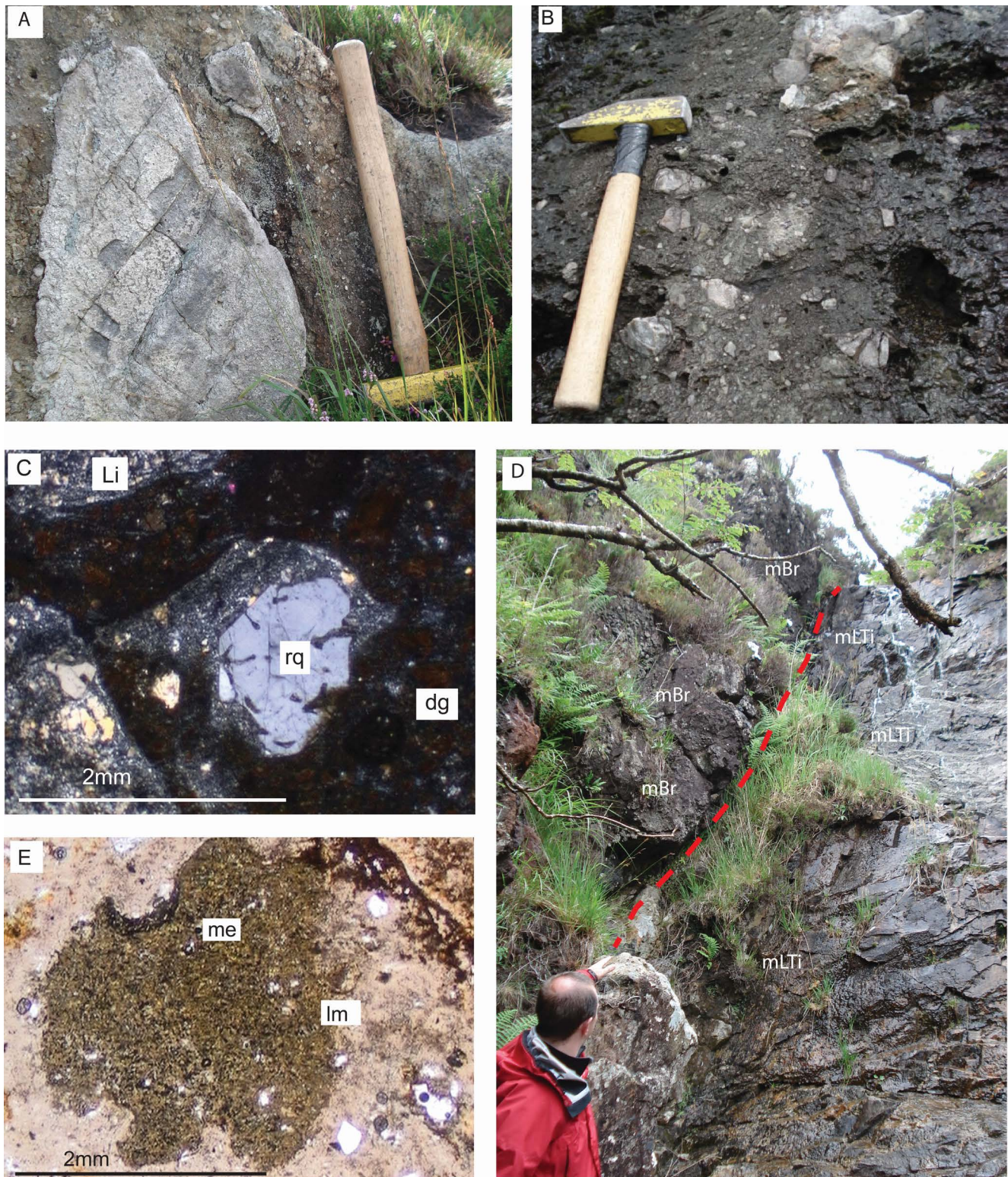


Figure 6: Field and petrographic characteristics of massive breccia (mBr) and massive lapilli tuff (mLT) [A] Quartzite block (hammer shaft 40 cm length) within matrix supported mBr at Cnoc nan Uan (log 9, 9 m: [Supplementary Material 1](#)). [B] Matrix supported ungraded mLT with an ash-granule grade matrix containing weathered in lithic-lapilli moulds (right of hammer). Note mechanical fracture of subangular quartzite lithic lapilli to right of hammer (log 16, 630m height, see [Supplementary Material 1](#)). [C] Secondary resorbed quartz (rq) within mLT overgrowing pre-existing lithics (Li). Devitrified brown glass (dg) is a common matrix feature. XP (log 13, 19 m height: [Supplementary Material 1](#)). [D] Matrix supported mBr in Allt nan Suidheachan (log 16, 500 m height, see [Supplementary Material 1](#)) containing blocks of arkosic sandstone, and incipiently welded mLTi. [E] Type III rounded matrix mafic enclave (me) [Troll et al. 2000; 2004] with highly irregular lobate margins (lm) in mLT (see log 18, 220 m height: [Supplementary Material 1](#)).

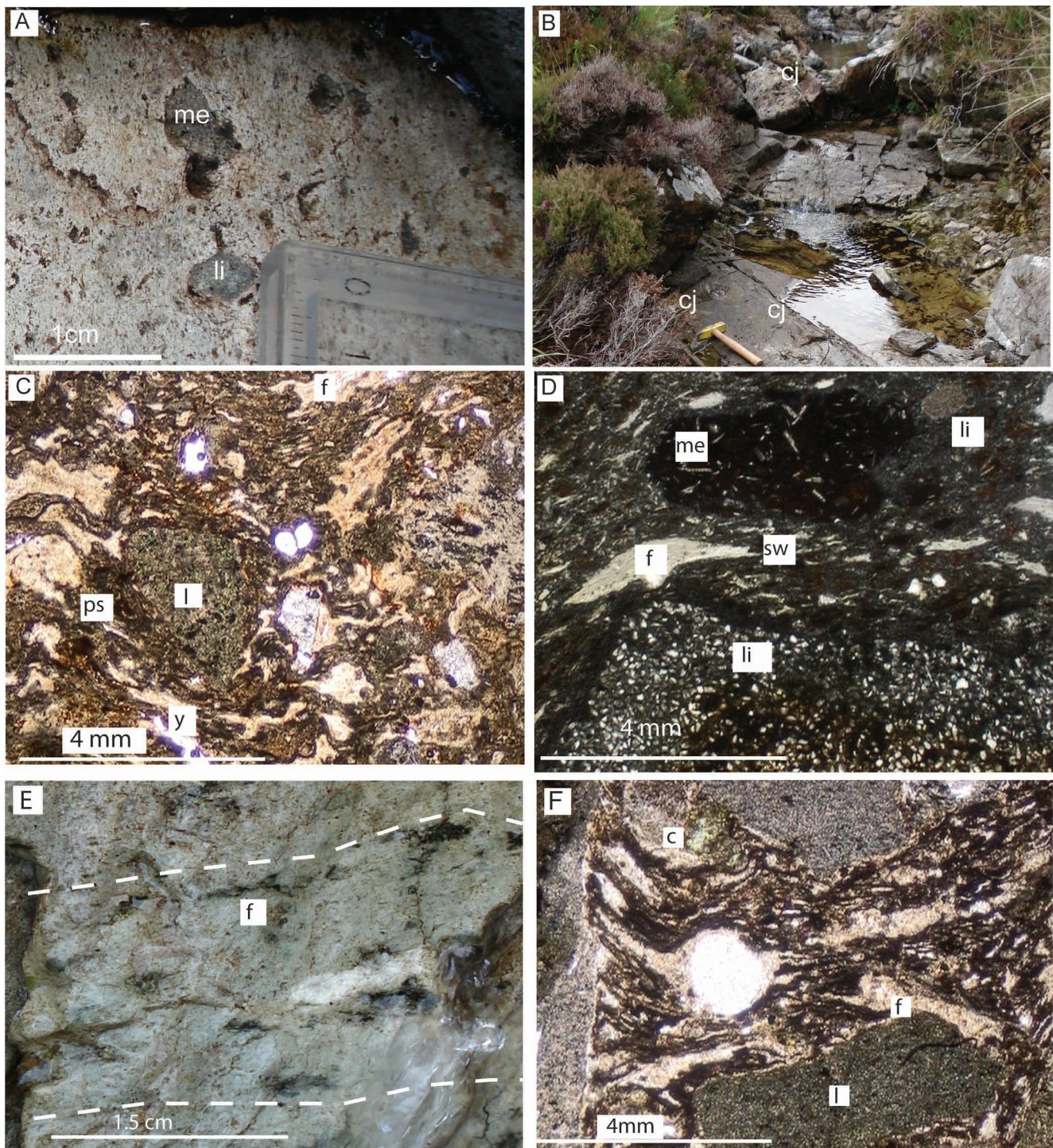


Figure 7: Field and petrographic characteristics of incipiently welded ignimbrite (mLTi) and welded ignimbrite (mLTe). [A] Type III mafic enclaves (after Troll et al. [2004]) are ubiquitous within mLTi as highly lobate clots <1.5 cm in diameter (log 16, 447 m height, see Supplementary Material 1). Lithic lapilli (li) are subrounded. [B] Near horizontally orientated columnar cooling joints (cj) in mLTi within Allt nan Suidheachan (log 16, 440 m height, see Supplementary Material 1). [C] Matrix of mLTi showing abundant undeformed-partially aligned glass shards (y). Left to right orientated fabric is deflected around a basalt lithic-lapilli (l). Much of the matrix is composed of very dark amorphous recrystallized glass. Matrix fiamme (f) are more deformed and streaked out towards top mid-page. Pressure shadows (ps) have formed around lithic lapilli (l) and within these regions fiamme are less deformed, PPL. (log 18, 292 m: Supplementary Material 1). [D] Heterolithic mLTi containing fine grained sandstone lithic lapilli (li), and fiamme (f) with swallow tail (sw) which together with external fabric has been deformed around the sandstone. A type III mafic enclave (me) with randomly orientated bytownite laths and lobate margins, also has fabric deflected around it. XP. (log 16, 445 m, Supplementary Material 1). [E] Eutaxitic fabric (white hatched lines) in mLTe orientated parallel to chloritized fiamme (f), log 14, 305 m height, Supplementary Material 1. [F] PPL image (log 16, 610 m height, see Supplementary Material 1) showing pronounced eutaxitic fabric within mLTe, chlorite (c), and fiamme (f), which have been deflected around lithic lapilli (l).

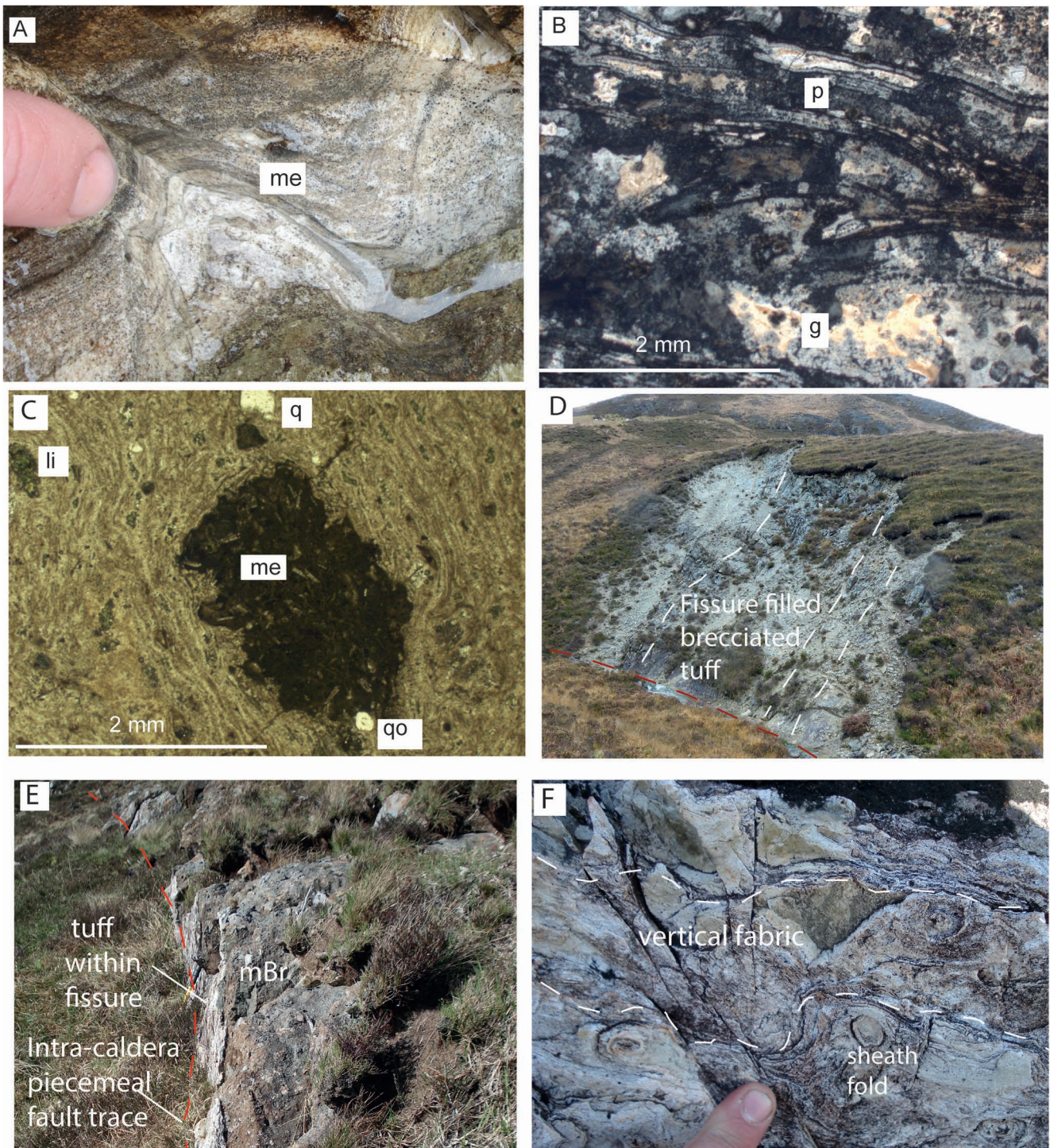


Figure 8: Field and petrographic characteristics of lava-like ignimbrite (mLT lava-like) and tuff filling fissures (TFF). [A] mLT lava-like, (log 18, 318 m height, see [Supplementary Material 1](#)). Note the dark and lighter coloured bands which reflect differences in mineral content (see [Figure 8B](#)), together with type II mafic enclaves (me), [Troll et al. 2004]. An orange weathered rind pervades to a depth of  $\leq 2$  mm. [B] XP image of parataxitic fabric (p) in quartz-rich recrystallised layers within mLT lava-like (log 18, 318 m height, see [Supplementary Material 1](#)). Note rod like terminations of parataxitic fabric, which appears as a series of rectangles. Undeformed glass shards (g), are evident in strain free regions (bottom middle). [C] PPL image of parataxitic fabric deformed around quartz (q), lithics (li), and type III mafic enclave (me), from log 18, 316 m height, (see supp file) in mLT lava-like. Late-stage quartz (qo) is seen overgrowing both mafic enclave and fabric. [D] Rhyolitic tuff filling a fissure with vertical fabric filling a 170 m long NNW-trending fissure in Allt Coire Forsaidh (log 12: [Supplementary Material 1](#)). Note near vertical fabric in tuff indicated by white hatched lines. [E] TFF. Rhyolitic tuff with vertical fabric filling a 170 m-long NNW-trending fissure (log 17: [Supplementary Material 1](#)). Note fault trace (red hatched line) which has offset fissure sidewall to produce step like profile. [F] TFF. Sidewall of fissure in [G], note the presence of vertical fabric (white hatched lines) and ubiquitous elliptical sheath folds.

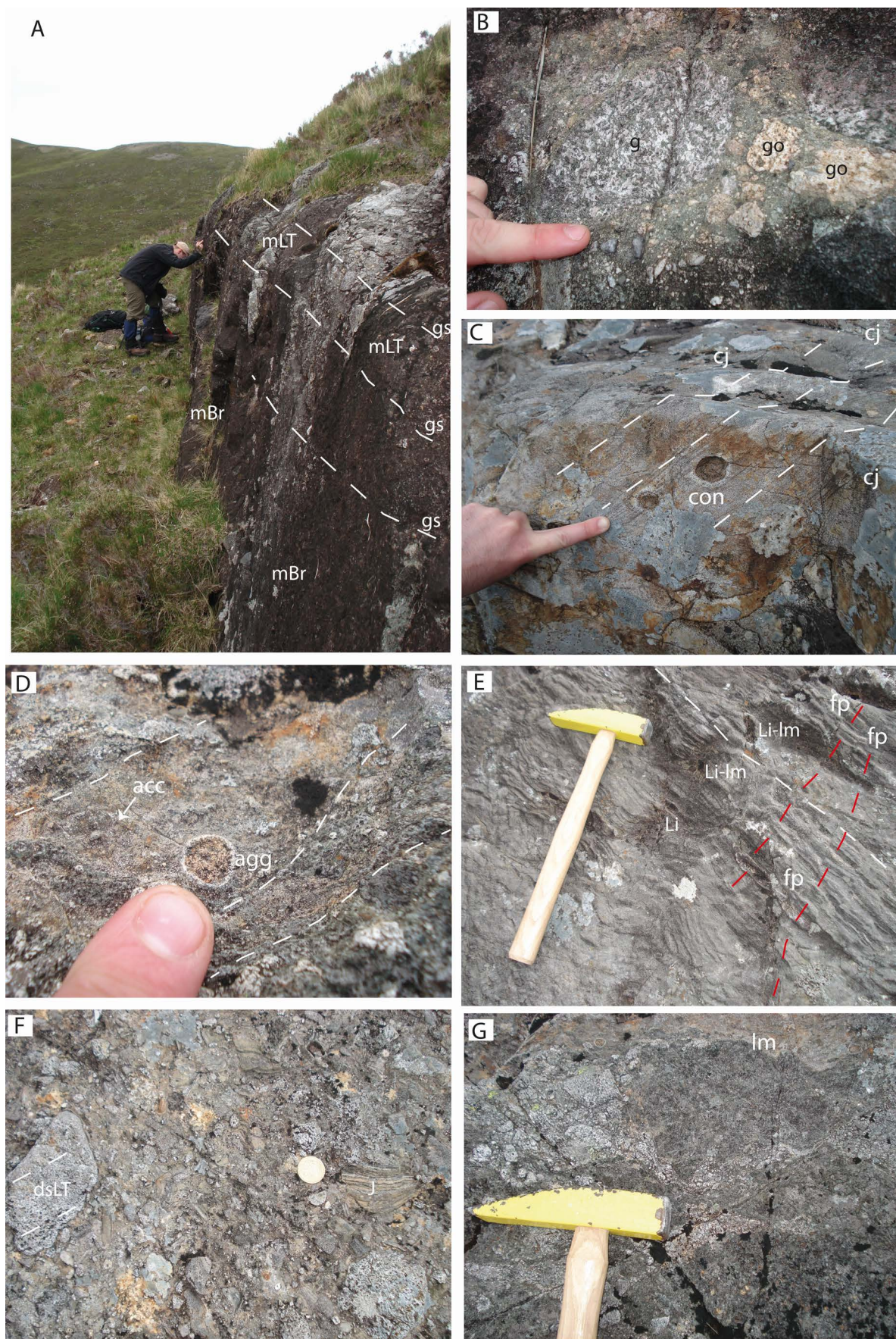


Figure 9: (Caption next page.)

Figure 9: (Previous page.) Field characteristics of extra caldera KVF ignimbrites at Belig. [A] Grading of lithic lapilli within mBr which grades up to mLT (finger indicating way up). The exposure face is gouged by glacial striations (gs). [B] subrounded granitic lithic lapilli within mBr in [A]. Some granitic lapilli (g) are chloritised, whilst other granite lapilli (go) have an orange hue, and are angular to subrounded. [C] Stratified tuff (sT) (NG 54301 24908) cut by NNE plunging cooling joints (cj), and containing post-depositional, sporadic, chloritised concretions (con), which overgrow fabric without displacing it. [D] Un-cored ash aggregates (agg) and sporadic accretionary lapilli (acc) within mLTacc (NG 54325 24866). [E] dsLT indicated by white hatched lines (at NG 54328 24646) containing mafic lithic lapilli (li) and mafic lithic lapilli with lobate margins (lm), together with angular rhyolitic lithic lapilli (all lithic lapilli  $\leq 5$  mm diameter). The exposure has been cut by faults (fp) which are denoted by red hatched lines. [F] Heterolithic matrix-clast supported mLT (NG 54308 24994) containing lithic lapilli of dsLT and bedded sandstone (J). [G] Heterolithic matrix supported mBr (NG 54345 24591) containing brecciated gabbroic blocks with lobate margins (lm) together with granitic blocks  $\leq 25$  cm in length.

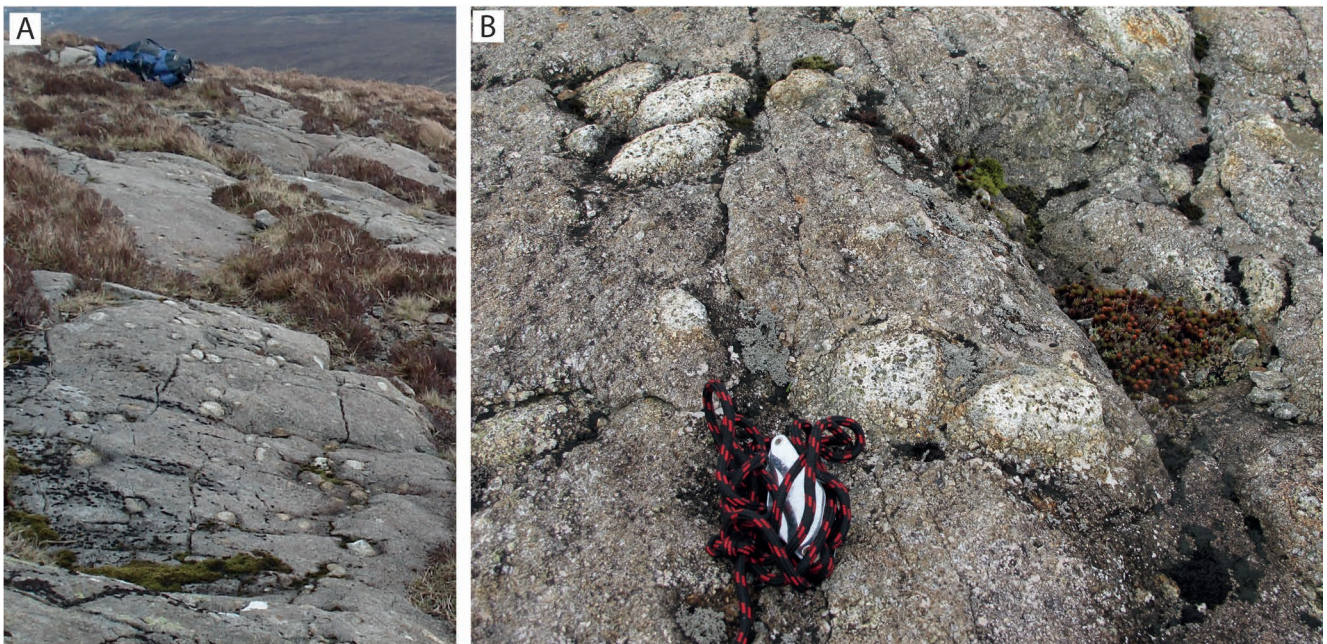


Figure 10: Field characteristics of silicic inclusions in basic intrusions. [A] Granitic inclusion bearing basic dyke from eastern summit flank of Ben Suardal [NG 63191 20477]. [B] subrounded granitic clusters within the basic dyke in [A].

up to 150 m in length and extend laterally along the coast for 2.5 km, implying a NW-trending fault representing the caldera outer margin is present immediately offshore [BGS 2005, Skye Central Complex, 1:25000 series]. We suggest that these faults delineate the NE caldera outer margin. Around Broadford and to the south and east of the Beinn an Dubhaich Granite, the caldera outer margin is likely coincident with the Kishorn Thrust trace. To the southwest the margin appears coincident with Loch Slapin and apparent discontinuities between Cambro-Ordovician and Jurassic rocks. Numerous extensional faults cut Lower-Middle Jurassic units interior to the caldera outer margin particularly NW and SW of the Eastern Red Hills Centre (Figures 2 and 3). Within the caldera outer margin, the substantial number of NW-trending fault traces which cut Jurassic, Cambro-Ordovician, and Neoproterozoic sedimentary rock (Figure 2) were probably associated with both caldera collapse, and the Paleocene regional stress field.

KVF ignimbrites also crop out outside of the NW caldera outer margin on Belig (Figures 2 and 9) and on top of the Marsco and Southern Porphyritic granites (Figure 2). Their

presence beyond the faulted outer margin provides evidence for at least part of the northern extent of the caldera structure and demonstrates that extra-caldera deposition occurred.

## 6 ERUPTION MODEL

In conjunction with the mapped lithofacies and caldera structural data, logs around the west (Figure 11) and south (Figure 12) of the Beinn na Caillich Granite (Figure 3) were correlated to establish four stages in an eruption model.

### 6.1 Pre-eruptive landscape

The pre-eruption geology of the area was dominated in the NW by the basic-ultrabasic Cuillin Centre, and the Western Red Hills Centre, and in the SE by Cambro-Ordovician dolostone and remnants of the Kishorn Thrust Sheet (Figures 13 and 14). Tectonically the region was active and was still under the influence of the regional scale Camasunary Fault and other extensional faults initiated in the Jurassic, whilst an extensional regime associated with North Atlantic spread-

ing, and an allied regional dyke swarm operated in tandem. Silicic and basic magma accumulated in the region and ultimately fed eruptions of the KVF (Figure 14). As magma was emplaced, tumescence occurred together with deformation of country rock. The nature of the magmatic plumbing system, contemporaneous deformation, and interaction with country rock is discussed in detail in Section 8 below.

## 6.2 Stage 1: Silicic eruptions, early caldera and inner ring-fault/dyke development

The first KVF deposits (Figure 15A) were produced by powerful, high vent mass flux eruptions which generated ~210 m of intercalated mLT and mBr in the south of the study area (Figure 3, log 16: Supplementary Material 1). Numerous repeating Stage 1 mLT and mBr units (logs Supplementary Material 1), indicate mass flux periodically waxed (mBr deposition), and waned (mLT deposition) throughout eruptions. We cannot rule out the possibility that these repeating mLT and mBr sequences may represent an earlier cycle(s) of caldera collapse since the paleosurface onto which they were erupted is not visible. Stage 1 eruptions were probably accompanied by the generation of an inner caldera ring-fault, and the start of ring-dyke intrusion. Magma mingling between basic and silicic magma produced hybrid magma which fed this ring-dyke, and resulted in incorporation of mafic enclaves throughout mLT and mBr matrix. Stage 1 PDCs were also sufficiently 'hot' to generate thermal spalling within mBr blocks (ash is frequently found between spalled layers) whilst rounding, and planar mechanical fracture within mBr blocks and mLT lapilli (Figure S3B) indicate that transportation took place within high-concentration granular currents [Branney and Kokelaar 2002] where collision of components was common. It is interesting to note that the only Jurassic sandstone blocks ( $\geq 70 \times 20$  cm) and lapilli found in the study area are contained within mBr which crops out at the very base of Stage 1 deposits (log 16, Supplementary Material 1). We tentatively suggest these Jurassic components may have been scavenged off a nearby Jurassic paleo-surface to the west around Allt Slapin (Figure 3), onto which the first PDCs were deposited. South of the developing caldera weak Mesozoic stratigraphic layers were further exploited by both silicic and then mafic pulses of melt which resulted in the formation of composite sills (silicic cores and basic margins; Figure 2).

## 6.3 Stage 2: Effusive volcanism

An abrupt change in both eruptive products and eruption style marked the end of Stage 1 volcanism as tapping of silicic melt stopped and a period of basic volcanism followed (Figure 15B). The most complete lava stratigraphy is in the south of the study area, and comprises four conformable lava flows (Figure 3, log 16, from 220 m: Supplementary Material 1). Lowest hawaiite flows crop out south and west in the study area and are succeeded by tholeiitic basalts (log 16 and Figure S11: Supplementary Material 1). However, in the west of the study area the lava flows display a different stratigraphy. The lowest hawaiite flow is succeeded by tholeiitic basalt, which is capped by mugearite (log 15: Supplementary Material 1). Although direct evidence is lacking, Stage 2 KVF lava flows were

probably fed by volcano tectonic faults and fissures generated by the NW–NNW Paleocene extensional trend. Individual flows may be separated by clay-rich paleosols (Figure 4A, B), or basic tuff horizons (log 16, 295 m height: Supplementary Material 1). This indicates that hiatuses of 100s–1000s of years occurred between flows [Retallack 1988], and that contemporaneous eruptions produced fall deposits between lava flows. Rare, localised, wet sediment and basic magma interaction took place towards the end of Stage 2 evidenced by peperite cropping out as laterally discontinuous lenses (log 16, 340 m height: Supplementary Material 1). Standing bodies of water were therefore present on the paleo-surfaces that some lava flowed over.

## 6.4 Stage 3: Fissure-fed, low boil over, high temperature eruptions

Stage 3 saw a return to explosive volcanism (Figure 15C); however, a hiatus existed between the end of Stage 2 and the start of Stage 3, as evidenced in the west of the study area where Stage 3 mBr cuts down into, and has incorporated, blocks of Stage 2 tholeiitic basalt (log 3, 29 m height: Supplementary Material 1). In the west of the study area the start of Stage 3 is marked by deposits of mLT and mLT<sub>e</sub> which crop out above Stage 2 mugearite flows (Figure 3, log 15, 160 m height: Supplementary Material 1). Succeeding intercalated mLT and mBr deposits are normally- reverse graded indicating fluctuations in terms of mass flux. These deposits are characterised by highly silicic groundmass content (Figure S12: Supplementary Material 1), and ubiquitous type II and III mafic enclaves [Troll et al. 2000; 2004]. The presence of such enclaves indicates that whilst Stage 3 is dominated by silicic ignimbrites some mafic melt was still introduced, and constantly stoked the conduit system. To the south of the study area Stage 3 was largely initiated and dominated by volumetrically dominant mLT<sub>i</sub> and high-grade fissure-fed mLT<sub>e</sub> and mLT lava-like. PDCs which generated mLT<sub>e</sub> and mLT lava-like were derived from fissure-fed fountains (Figures 7 and 8 and Supplementary Material 1 Figure S10). We suggest such fissures were generated either by magma chamber tumescence, regionally associated extensional fractures, or both. In several localities within the inner ring-fault, high-grade ignimbrites are in extremely close proximity to regionally aligned NW–NNW-trending fissures. Rapid burial allied with the low height of fissure-derived tuff fountains, ensured that the PDCs they would have fed remained at temperatures ~1000 °C [Andrews and Branney 2011]. At such temperatures PDCs were syn- to post-depositionally welded and agglutinated, before the deposit cooled back through the glass brittle–ductile transition zone [Freundt 1998; Russell et al. 2003]. The temperature of PDCs which produced mLT-lava-like deposits could also have been further increased by up to 250 °C by 'strain heating' associated with syn- to post-depositional shearing [Robert et al. 2013].

Stage 3 lava-like ignimbrites (logs 7, 13, 16, and 18: Supplementary Material 1) may conformably succeed mBr (log 7, 11 m height: Supplementary Material 1), or mLT (log 13, 8 m height: Supplementary Material 1) which indicates that Stage 3 was characterised by extreme unsteady state eruption

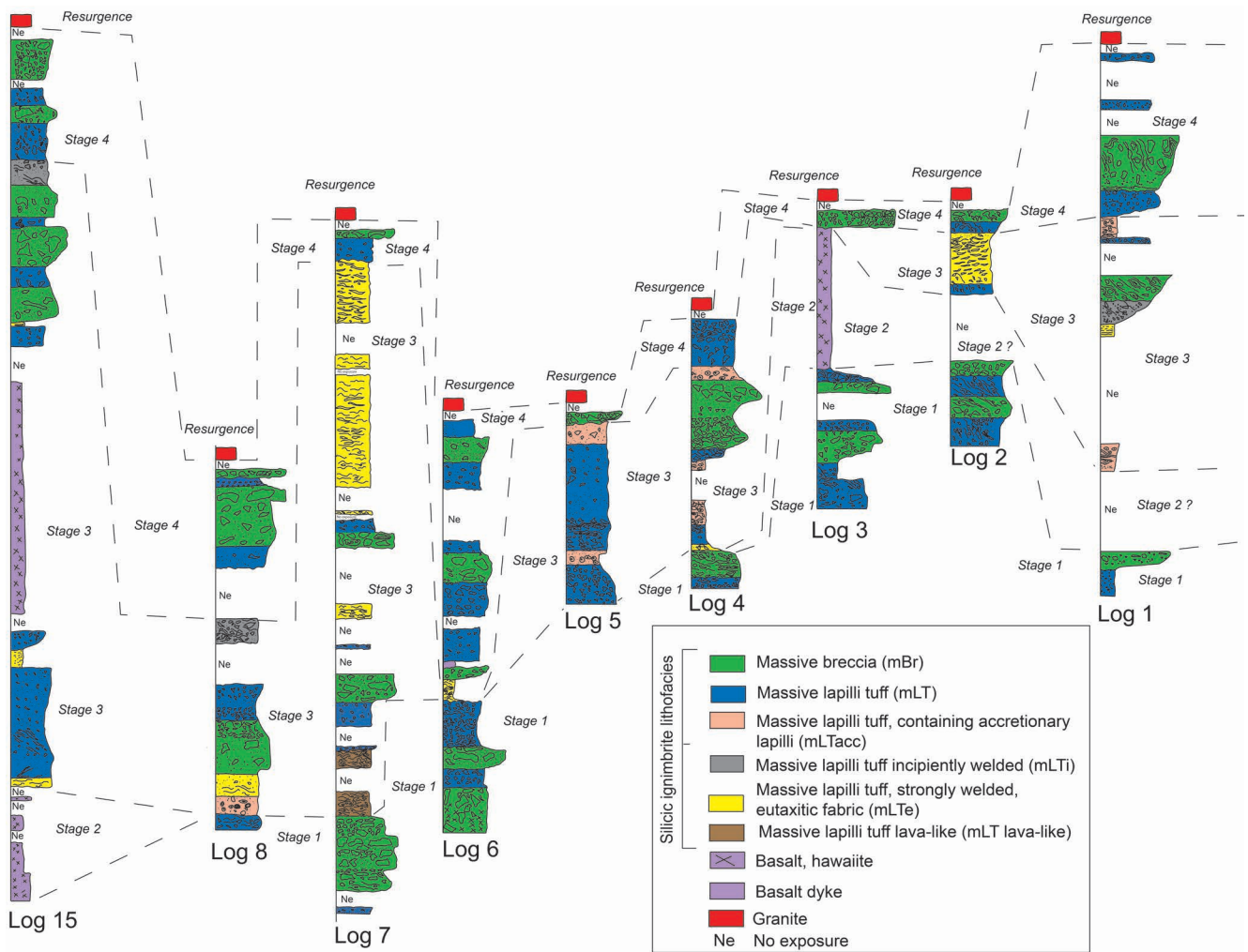


Figure 11: Correlation of logged sections (west). Proposed KVF eruption stages interpreted by correlation of logs 1–8 and 15 to West of Beinn Dearg Bheag (Figure 3). Generalised vertical scale shown may be reduced in regions of no exposure (for details of vertical scale within individual logs 1–8 and 15 refer to Supplementary Material 1 (logs A)).

dynamics, and highly fluctuating mass flux volumes. Within the Kilchrist Caldera some fissures were ‘re-exploited’ by later NNW basic dykes of the regional swarm since they chill into, and are juxtaposed with, fissure fed tuff (Figure S10E). Fissures filled with tuff which fed PDCs are also evident within the outer marginal zone east of Beinn na Caillich (Figure 2). Sporadic outcrops of mLT<sub>e</sub> (probably generated during Stage 3 KVF) within the outer marginal zone, south east of Loch Kilchrist (Figure 2) suggest Stage 3 PDCs ran out in a south east direction from the inner ring fault. Stage 3 KVF mLT<sub>acc</sub> and sT cropping out at Belig also represent extra-caldera deposits, and suggest NW directed runout also took place (Figure 2).

Throughout Stage 3 eruptions the presence of mafic enclaves shows mafic melt continued to be tapped from a sub-surface source(s) and mingled with silicic melt. There is a clear increase in the quantity and size of matrix mafic enclaves between Stage 1 and Stage 3 KVF eruptions which is evident at both macro, and micro scale. The only Stage 3 lava recorded is a mugearite flow, which crops out in the west of the study

area (log 15, 110 m height: Supplementary Material 1). The bulk chemistry of this mugearite is similar to that of type III mafic enclaves found within Stage 3 mLT deposits, (Figure S11: Supplementary Material 1). Such chemical affinities suggest the same mafic source produced both the mugearite and mafic enclaves. Sporadic, thin, stratified tuff (sT) fall deposits cut by columnar cooling joints (Figure 5A, B) punctuate Stage 3 eruptions (log 9, 3 m height: Supplementary Material 1). Fine-grained laminations within this stratified tuff indicate deposition was generated via direct fall from eruption ash clouds, whilst contractional cooling joints indicates ash was deposited hot. Loading structures, cross stratification and micro-faults indicate post-depositional reworking took place.

Elsewhere within the NNW margin, outer marginal zone basalt flows crop out on the northern flanks of Beinn na Cro (Figure 2). Since these basalts are intruded by apophyses of granite [Smith 1958] they must pre-date granite intrusion. The Beinn na Cro basalts were probably supplied via intra caldera faults and NNW-trending fissures associated with regional Pa-

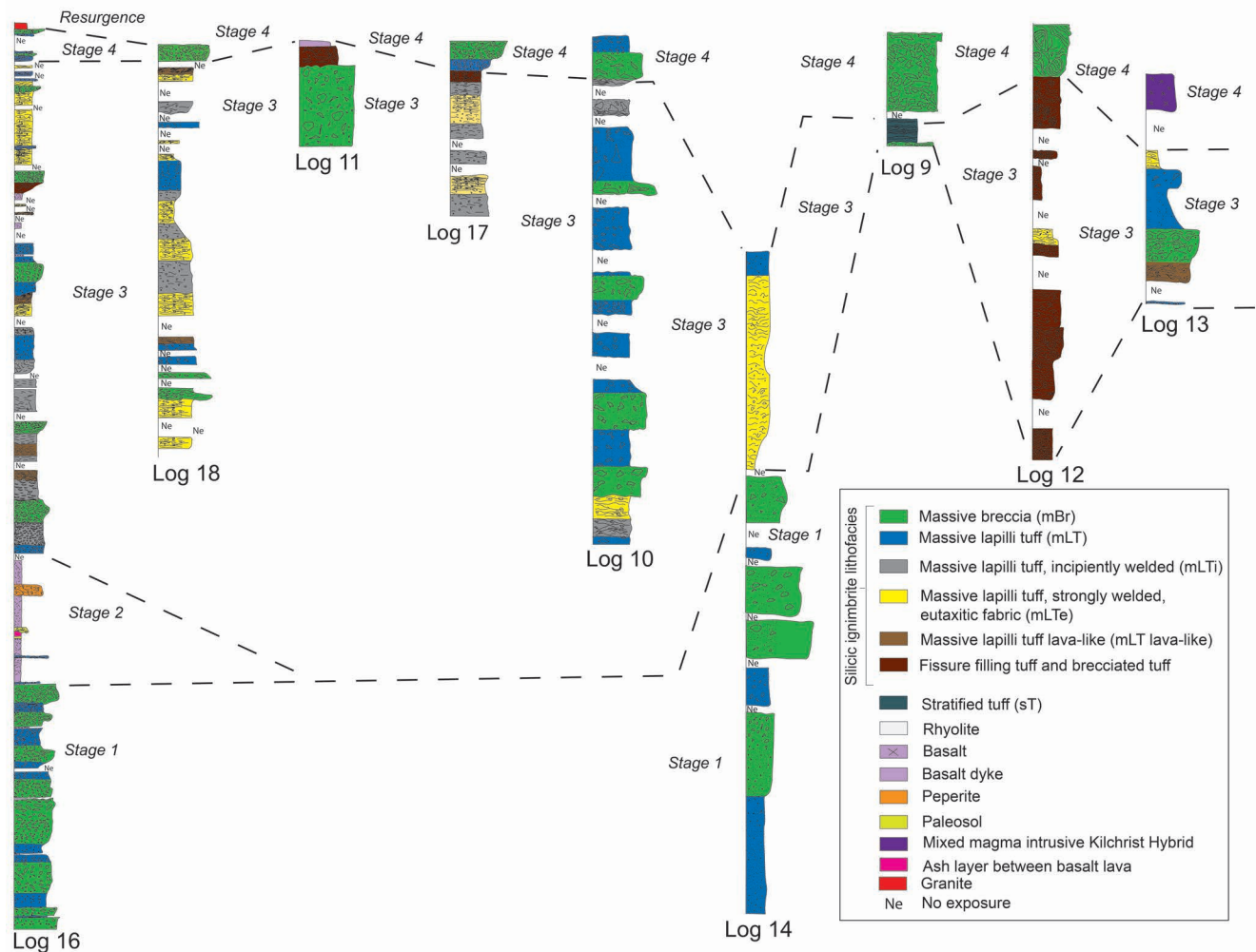


Figure 12: Correlation of logged sections (south). Proposed KVF eruption stages interpreted by correlation of logs 9–14 and 16–18 to the South of Beinn Dearg Bheag (Figure 3). Generalised vertical scale shown may be reduced in regions of no exposure (for details of vertical scale within individual logs 9–14 and 16–18 refer to supplementary file (logs B)).

leocene extension during Stage 3 (although we cannot preclude Stage 2) of KVF eruptions (Figure 15C).

#### 6.5 Stage 4: Catastrophic collapse, accumulation and choking of magmatic system

A distinct change in both eruption style and a substantial increase in mass flux marked the start of Stage 4 (Figure 16A). High-energy, non-steady-state eruptions produced repeating mBr and mLT units which cut down into Stage 3 mLTe, mL-Tacc and mLT lava-like deposits (logs 1, 5, 6, 7, 12, 15, 16, and 17 Supplementary Material 1). Such mLT and mBr units frequently grade into each other both laterally and vertically, over a few metres. Eruption dynamics changed from Stage 3 fissure fountaining to more column-driven eruptions as Stage 4 caldera collapse proceeded. Allied volcano-tectonic faulting resulted in caldera floor piecemeal block faulting, as mass flux built to a crescendo. Syn-tectonic subsidence of mBr during Stage 4 ground shaking and magma evacuation, is indicated by abrupt changes in unit thicknesses, across fault traces, throughout the study area, for example around Meall Coire Forsaidh, Cnoc nan Uan, Cnoc nan Fitheath, and Allt Slapin

(Figure 3). Randomly orientated fault traces (typically ~1 km in length), surround the Beinn na Caillich Granite and cut country rock within the caldera outer marginal zone (Figure 2). Such faulting indicates significant piecemeal caldera floor collapse events took place. Caldera collapse did not extend south of the Kishorn Thrust (Figure 2) which suggests that inward subsidence was constrained by this structure. The collapse of the subsiding caldera margin was linked to exploitation of both silicic and basic magma fractions which likely supplied magma for the Eastern Red Hills Outer Granites (Glas Bheinn Mhor, Beinn na Cro, and Creag Strollamus), and gabbros (Beinn na Cro and Broadford). The relative ages of intrusion between these granites and gabbro are complex, and it is difficult to determine a clear pattern of the order of magmatic tapping. Mafic enclaves and other disequilibrium textures are ubiquitous throughout Stage 4 mBr and mLT and indicate that magma mingling continued during the final cataclysmic collapse related eruptions. Mafic clots are also common within the Kilchrist Hybrid Ring Dyke which probably further intruded, and exploited, ring fractures during the collapse stage. The preserved composite sills with silicic cores ~50 m thick

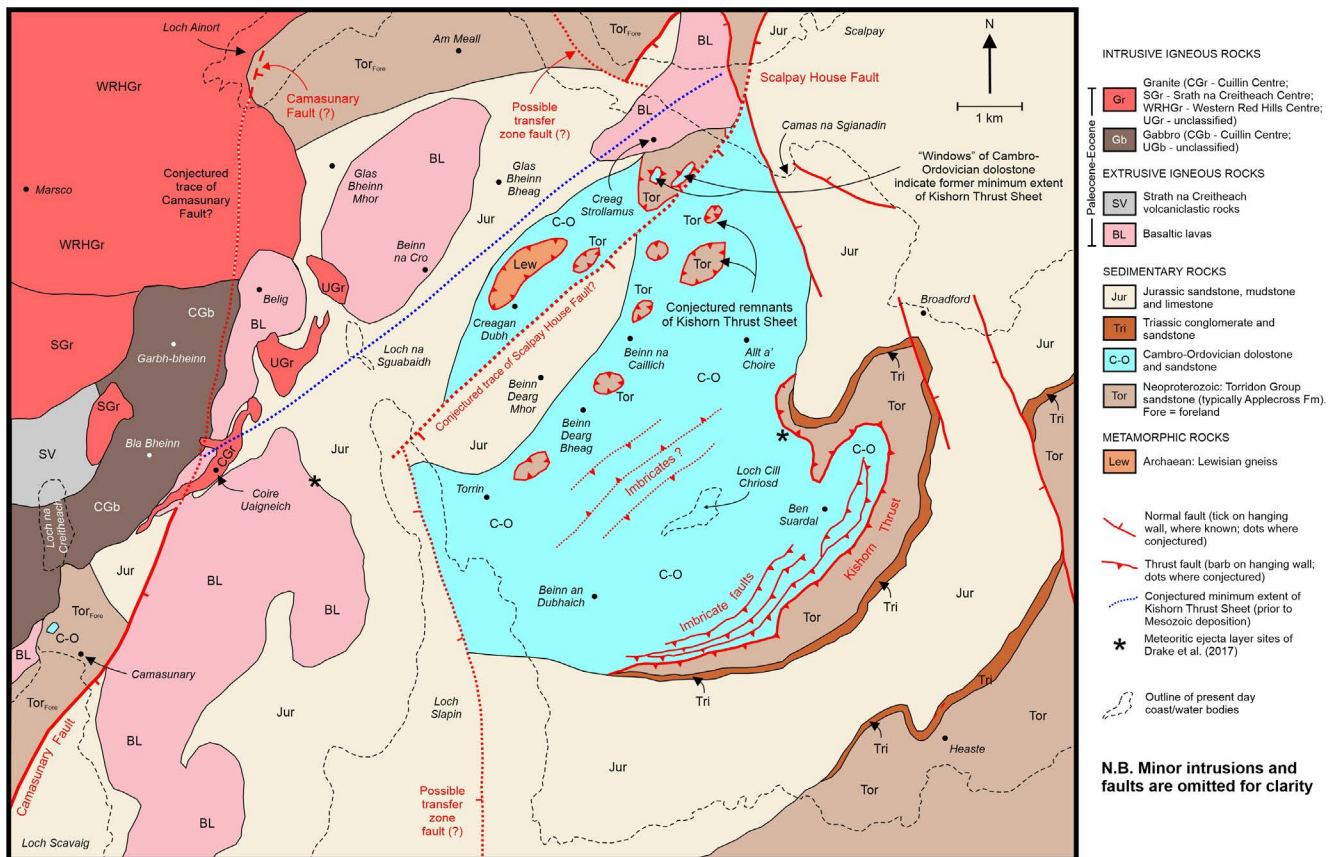


Figure 13: Schematic map of the paleo-landscape at ~58 Ma.

[Emeleus and Bell 2005] indicate that magma throughflow was volumetrically substantial.

Stage 4 mBr and mLT units are frequently cut by faults (Figure 3) and juxtaposed with different ignimbrite lithofacies. Block sizes within Stage 4 mBr are also greater than in any other mBr deposits found in earlier eruption stages. Additionally, Stage 4 mBr is overwhelmingly reverse graded (logs 1, 2, 5, 7, 8, 9, 12, 15, 17, and 18: Supplementary Material 1). Mass flux was therefore at its greatest during the latter parts of Stage 4, and proximal breccias containing large lithic blocks were deposited via high energy PDCs. Temporally this juncture probably coincided with catastrophic caldera collapse. The lack of 'high grade' ignimbrite within Stage 4 indicates agglutination and coalescence was no longer supported as PDCs became choked with blocks from either a collapsing caldera wall, or caldera floor blocks. At a micro-scale the mechanical fracture of both crystals, and blocks, within Stage 4 mBr indicates eruptions were high in mass flux, and that subsequent PDCs were high in block concentration, which resulted in substantial deposits of clast supported mLT, and mBr (logs 1, 5, 6, 7, 12, 15, 16, and 17: Supplementary Material 1). Some of these PDCs ran out ~6.5 km north past the caldera outer margin to Belig where mLT and mBr was deposited onto a pre-existing gabbroic and granitic topography (Figures 2 and 9). Scavenging of the paleo-surface by these PDCs resulted in incorporation of gabbro and granitic blocks. Such ignimbrites were probably preserved because they filled paleo-depressions.

## 6.6 Resurgent Phase

Following caldera collapse, a resurgent period occurred (Figure 16B), and the Eastern Red Hills Inner Granite of Beinn na Caillich, Beinn Dearg Bheag, and Beinn Dearg Mhor was intruded. (Figures 2 and 3). The granite is near circular in profile, steep sided, and interpreted as a "true" resurgent phase which completely post-dated Stage 4 caldera collapse. Field evidence confirms that the intrusion of this granite post-dates ignimbrite deposition since Jurassic sedimentary rock is rucked up (and dips), towards the western margin of Beinn Dearg Mhor (Figure 3), whilst xenolith 'rafts' (1 × 1.5 m) of ignimbrite (mLTi) are wholly enclosed by granite south east of Beinn na Caillich (NG 60702 22363). It is possible that resurgent effusive activity (e.g. lava domes) took place, but no such evidence is preserved.

## 7 GEOCHRONOLOGY OF THE KILCHRIST CALDERA AND ITS IMPLICATIONS

During the present study, U-Pb dates were acquired from zircons in targeted areas to try and constrain Paleocene caldera generation, collapse, and subsequent Eastern Red Hills resurgence (Figure 17). The presence of granite inclusions contained within a basic dyke near the summit of Ben Suardal dated during this study at  $56.45 \pm 0.19$  Ma (Figure 2, 10A, B, 17A, B, and Supplementary Material 1) suggests that a hitherto unidentified silicic reservoir was resident immediately beneath or laterally close to Ben Suardal, prior to the onset of the

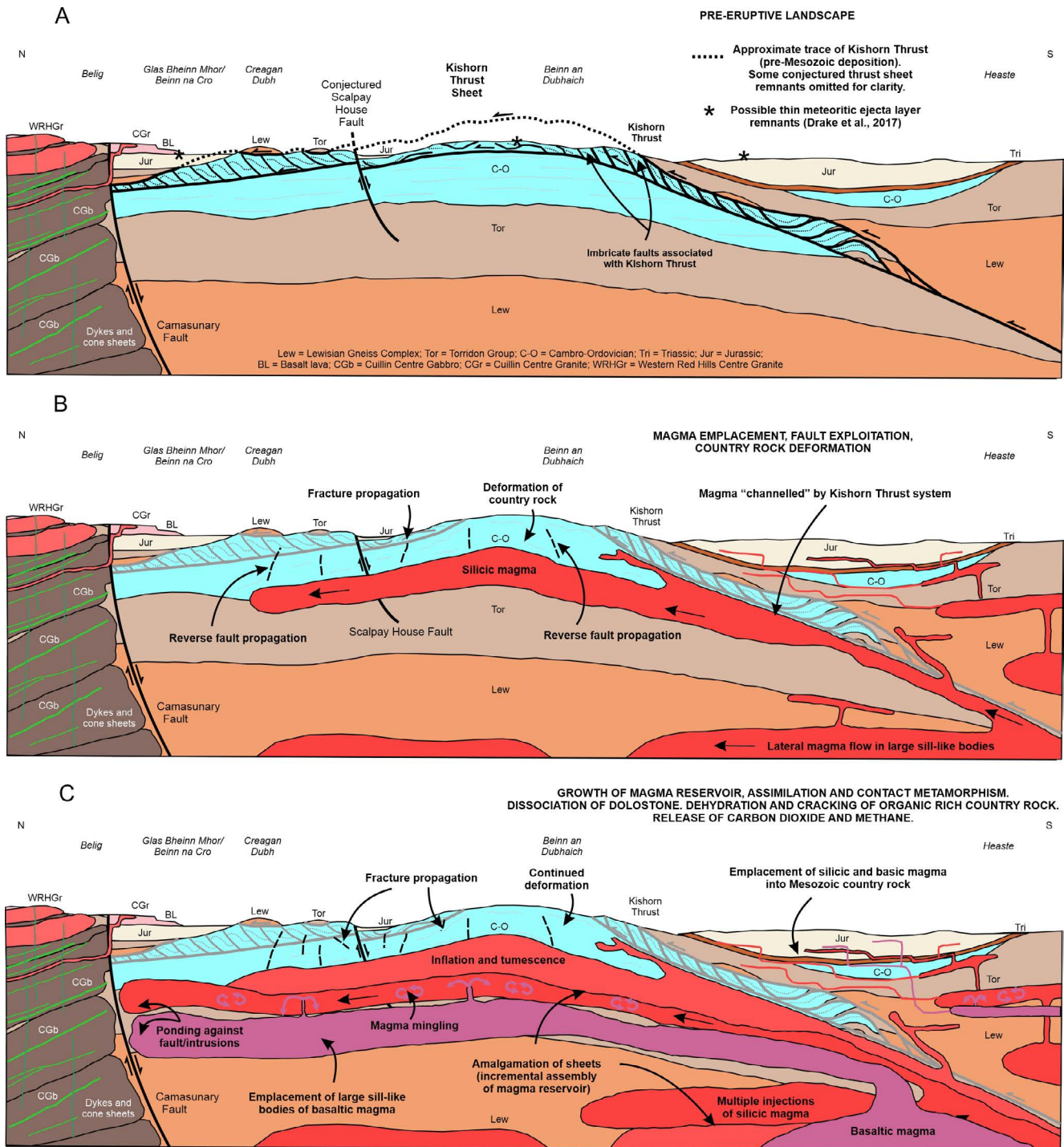


Figure 14: Schematic models of the pre-eruption subsurface. [A]–[C] Pre-eruption geology showing the Cuillin Centre as a physical barrier to northerly magma migration and the exploitation of the Kishorn Thrust zone, and Mesozoic strata by both silicic [B] and basic [C] magma.

volcanic episode. Within the inner caldera ring-fault zircons from Stage 3 incipiently welded ignimbrite yielded an average age of  $56.15 \pm 0.19$  Ma (Figure 17C, D, log 16, height 490m, and Supplementary Material 1). This date is coincident with the Paleocene Eocene Thermal Maximum (PETM) [Turner 2018]. The Beinn an Dubhaich Granite was emplaced into the collapsing caldera margin at  $55.89 \pm 0.15$  Ma [M. A. Hamilton, in Emeus and Bell 2005]. The KVF was then intruded by the

resurgent Beinn na Caillich Granite before pitchstone dykes intruded the granite at  $55.7 \pm 0.1$  Ma [M. A. Hamilton, in Emeus and Bell 2005] (Figure 2). These dates indicate that subsurface silicic magma chamber(s) were present beneath the current position of Ben Suardal and Beinn an Dubhaich (Figure 17C, D) at  $56.45 \pm 0.15$  Ma. The volcanic episode followed shortly after, with Stage 3 eruptions dated as  $\sim 56.15 \pm 0.19$  Ma. Eruptions continued throughout the PETM until the Beinn an

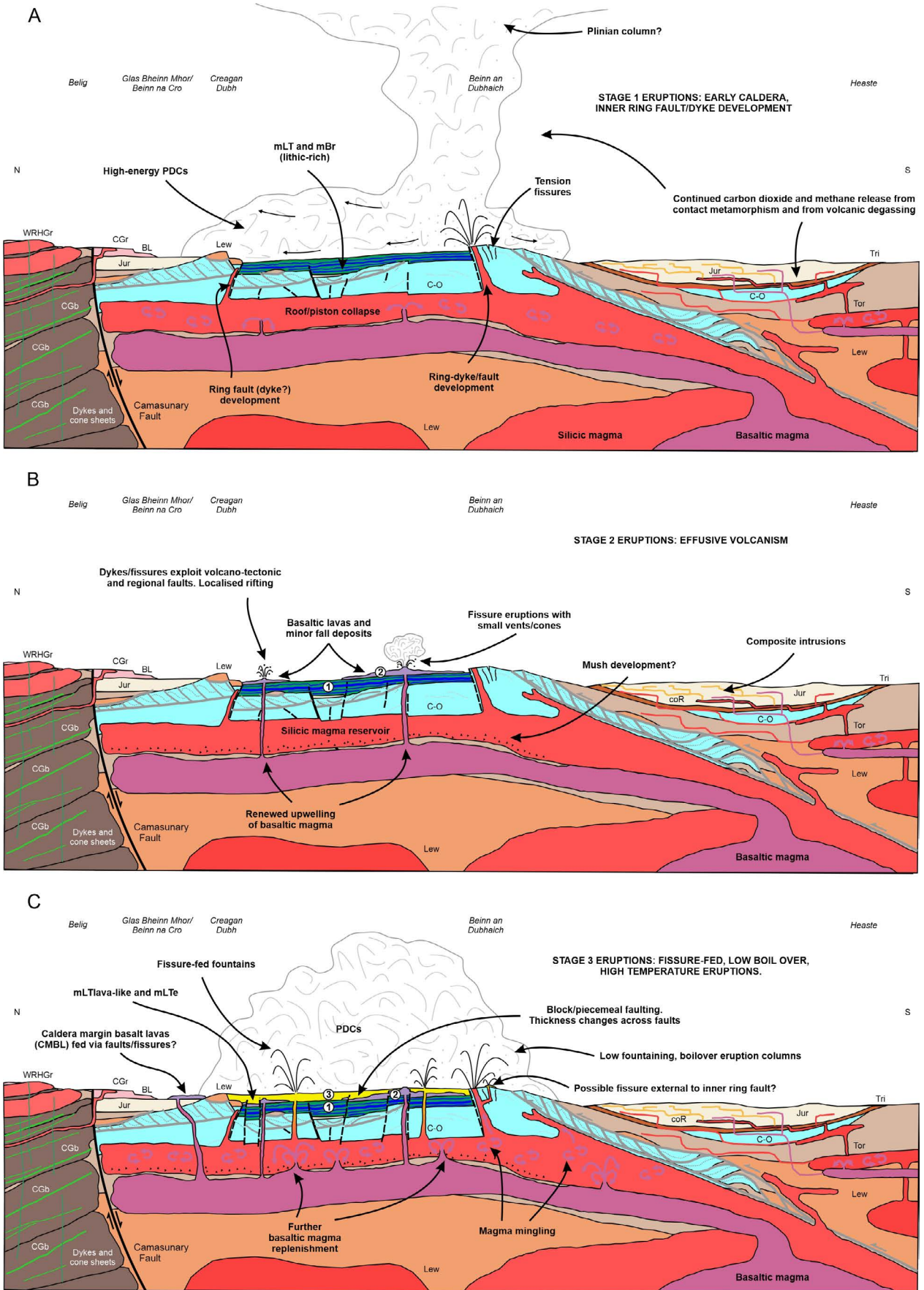


Figure 15: Stage 1–3 of KVF eruptions. [A] Early caldera, inner ring-fault and dyke development. [B] Effusive volcanism. [C] Fissure fed, low boil over, high temperature eruptions.

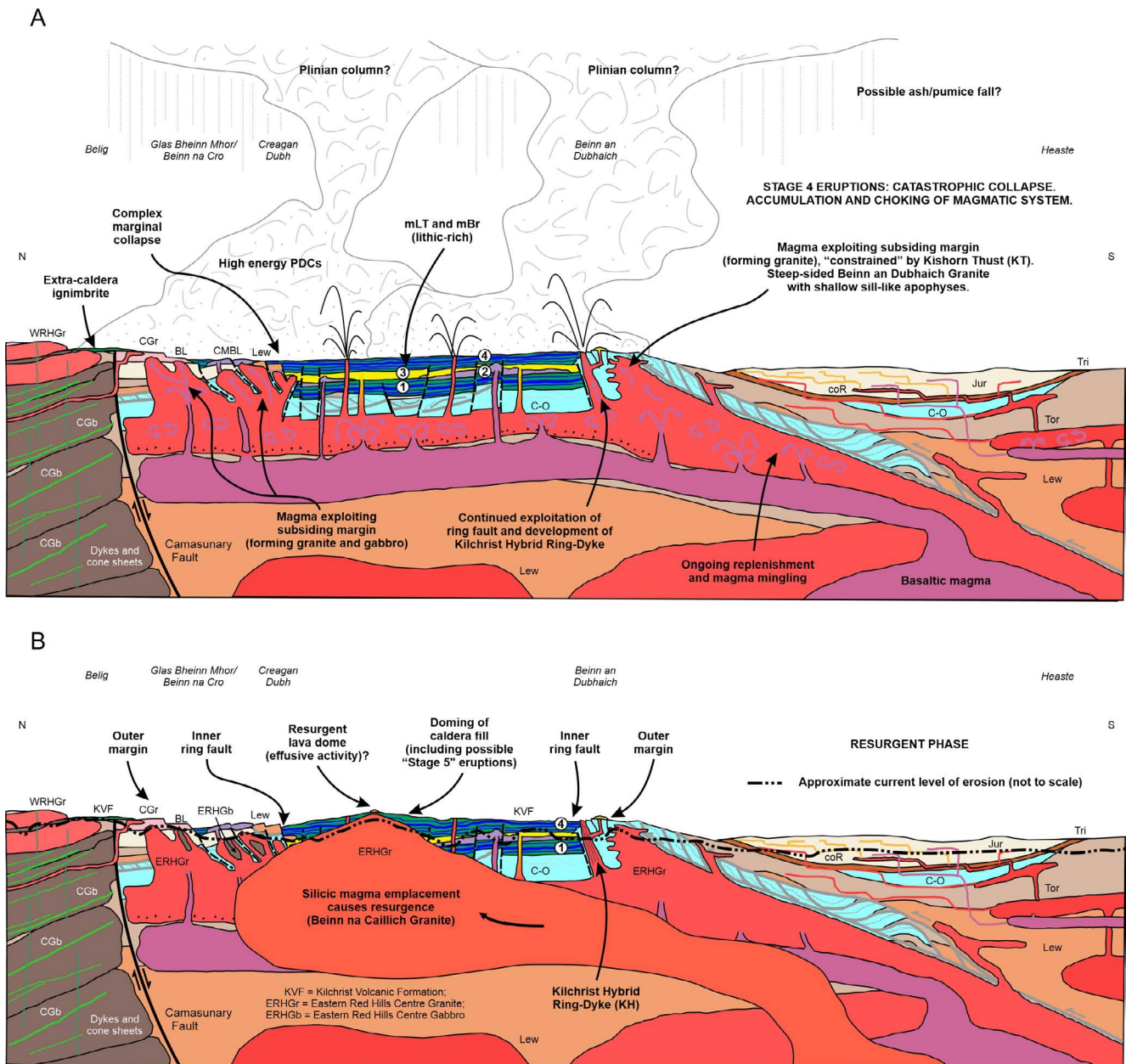


Figure 16: Stage 4 of KVF eruptions. [A] Caldera collapse and choking of magmatic system. The subsequent [B] resurgent phase resulted in emplacement of the Beinn na Caillich granite.

Dubhaich and Beinn na Caillich granites were emplaced at ~55.89–55.7 Ma. These dates indicate the volcanic episode and subsequent resurgence spanned about ~0.5 Myr. Such rapid volcanic and intrusive episodes are evident elsewhere in the BPIP, for example Rum, where volcanism, caldera collapse and resurgent central complex intrusion took place over a similar timeframe ~0.5 Myr [Hamilton et al. 1998; Troll et al. 2000; Chambers et al. 2005].

## 8 DISCUSSION

### 8.1 Caldera-related faults/subsidence, proximal caldera collapse deposits, nature/duration of eruptions, magma mingling, and resurgence

Numerous caldera collapse related faults are orientated approximately “radially” around the Benn na Caillich Granite

(Figure 2). These faults cut either Archean gneiss, Neoproterozoic Applecross sandstone, Ordovician dolostone, Lower-Upper Jurassic sedimentary rocks, or Paleocene basalt [see BGS 2005]. The complex juxtaposition of different lithologies indicates both the likely variable nature of the pre-collapse surface, and differential collapse during caldera formation. Radial faults cut both the inner ring-fault, and outer marginal zone (Figure 2), and indicate the caldera was faulted by piecemeal subsidence [Moore and Kokelaar 1997; Troll et al. 2004]. To the south and SE of the caldera outer margin, the Kishorn Thrust and older country rocks are faulted in a NW–NNW orientation, and offset in a NW–SE orientation. These faults also have an E–NE down-throwing extensional component (Figure 2). In a similar manner composite Paleocene composite sills south of the Kishorn Thrust have been offset by NW–

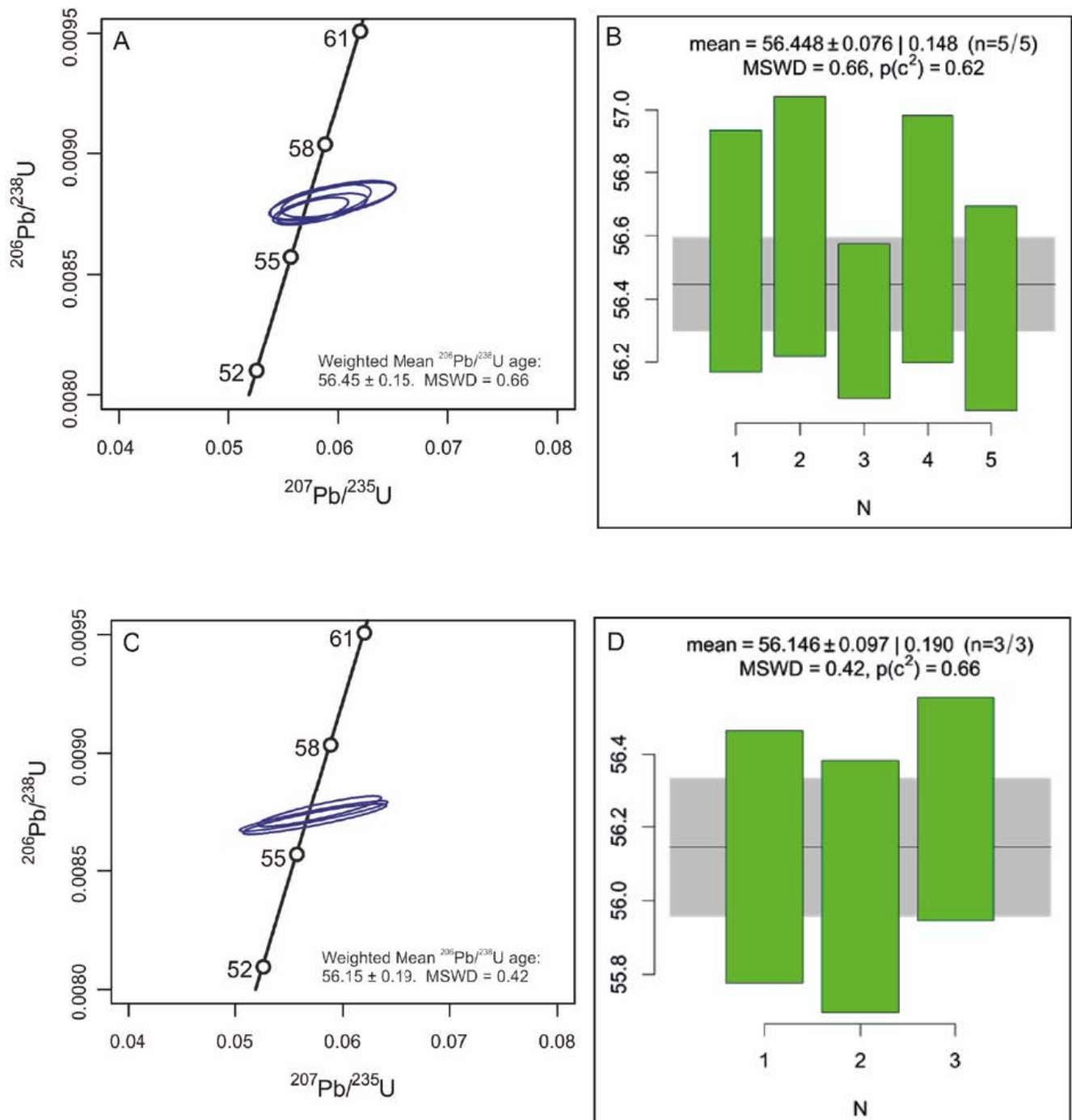


Figure 17: Results of U-Pb dating of zircons using chemical abrasion isotope dilution thermal ionisation mass spectrometry (for full details of methodology refer to [Supplementary Material 1](#)): [A] 95 % confidence ellipses for zircon ages within granitic inclusions on Ben Suardal (NG 63191 20477). [B] Weighted average dates for zircons in [A] (NG 63191 20477). [C] 95 % confidence ellipses for zircon ages from Stage 3 KVF mLTi at Allt nan Suidheachan (NG: 59618 20783) see ([Figure 3](#), log 16, 445m height, [Figure S1](#), [Supplementary Tables 2–6](#): [Supplementary Material 1](#)) [D] Weighted average dates of zircons in [C] (NG: 59618 20783).

NNW-trending faults, and downthrown to the ENE ([Figure 2](#)). This evidence suggests extensional faulting was contemporaneous with/post-dated sill intrusion and solidification.

The broadly oval-shaped fault traces of the inner ring-fault and the outer margin ([Figure 2](#)) are similar to the Glencoe Caldera profile [[Clough et al. 1909](#)], and many other calderas worldwide. The southern margin of the inner ring-fault is

marked by the incomplete, semi-arcuate Kilchrist Hybrid Ring Dyke, which does not crop out in the north. The volume of KVF caldera-fill inside the inner ring-fault is considerably greater than the small, isolated exposures found in the outer marginal zone and outside the caldera. This indicates that the greatest amount of subsidence occurred inside the ring-fault, delimiting a block of crust that probably collapsed initially as

a piston, but then broke up in more complex piecemeal fashion. Scant ignimbrite exposures crop out in the outer marginal zone, which presumably was subjected to more erosion and dyke intrusion than down-dropped KVF within the inner ring-fault.

The KVF is the thickest preserved caldera series thus far documented within the BPIP (Figure 3, see A–B line of section). However, the total thickness of KVF deposits could be greater because the contact between the first erupted deposits and paleosurface is missing. Lithic-rich lapilli, and block breccias, commonly form proximal intra-caldera deposits, and whilst often poorly preserved, are recorded in both modern and ancient caldera settings [Brown et al. 2009; Smith and Kokelaar 2013; Jordan et al. 2018]. In the KVF the typically large block size of mBr close to Eastern Red Hills granite provides an impressive record of proximal caldera collapse-related deposition. In most studies of intra-caldera proximal deposits, coarse lithic breccia ignimbrites are typically only a few metres thick and are considered to record catastrophic collapse events [Smith and Kokelaar 2013; Jordan et al. 2018]. In the KVF mBr is ubiquitous and can be tens of metres thick, indicating that the eruptions were extremely high-energy, frequent, and *relatively* prolonged. The presence of thick, coarse, mBr units in Stages 1, 3, and 4, indicates both that these catastrophic collapse events likely occurred throughout the history of the Kilchrist Caldera, and highlights the plentiful availability of coarse lithic material for scavenging by PDCs. Reverse grading in mBr units indicates vent mass flux was increasing towards the latter parts of eruptions, and likely contemporaneously with piecemeal caldera floor faulting and collapse of caldera wall. We tentatively suggest that the KVF eruptions are unique in their preservation of such coarse ignimbrites as we know of no other calderas where such coarse primary pyroclastic materials are so dominant.

Some workers have previously suggested that pyroclastic deposits at Kilchrist were reworked as a result of intrusion-driven uplift [Bell 1985; Bell and Harris 1986]. Whilst we cannot rule out some post-eruption reworking of mLT and mBr, the presence of heat-derived features (thermal spalling of blocks, block lobate margins, cooling joints in select units, lithophysae) strongly indicates that the majority of mBr and mLT was deposited via ‘hot’ PDCs. Other factors argue against mBr and mLT being reworked sedimentary deposits, for example reverse grading of blocks is extremely common within mBr, but such grading is very poorly developed in debris flow deposits [Blair and McPherson 1998].

A further characteristic of the KVF is the apparent scarcity of fall deposits. This could be explained by the poor preservation potential of such fine ash and/or pumice-rich deposits or could reflect the style of volcanism that operated during eruptions. Where lava-like ignimbrites are associated with collapse calderas there is often a scarcity of associated fall deposits. This is because PDCs are generated from low height flaring fissures, and not high eruption columns, that typically generate associate fall deposits [Freundt 1998]. In Stage 3 KVF lava-like ignimbrites are preserved and geographically widespread (Figure 3). However, scarce fall deposits occur in the west of the inner ring-fault, where accretionary lapilli

are preserved within mLTacc units (Figure 3, logs 1, 4, 5, and 8: Supplementary Material 1). Such mLTacc units indicate the periodic development of higher eruption columns or “phoenix plumes”, where ash aggregates developed before falling into underlying low particle concentration PDCs [Brown et al. 2010]. The dominant mLT and mBr of stages 1, 4, and part of 3, would normally suggest the presence of substantial Plinian-style eruption columns. It is possible that the anomalously coarse lapilli- and block-rich nature of these deposits suppressed eruption column heights, and/or the density currents involved were extremely high-energy and erosive, again due to lithic content, therefore destroying any fall deposits that had been generated. Within the KVF, the only ‘true’ fall deposit preserved is a stratified tuff from Stage 3, cropping out at Cnoc nan Uan (Figure 5A, B). This thinly laminated unit displays evidence of minor subaqueous reworking, perhaps indicating deposition in a small body of water, which may have enhanced its preservation potential.

In attempting to constrain the stratigraphy, timing, and duration of the KVF-forming eruptions we have classified the earliest repeating mLT and mBr sequences (log 16: Supplementary Material 1) as Stage 1 KVF deposits. We cannot determine the full extent/thickness of these deposits due to lack of exposure, and lack of contact with the caldera floor. Older, separate, caldera collapse phases may therefore be present beneath our KVF Stage 1 deposits. Succeeding Stage 2 KVF tholeiitic lava flows are separated by paleosol horizons  $\leq 5$  cm thick (Figure 4A, B, log 16: Supplementary Material 1). These probably represent diastems of  $\sim 50$ – $100$  years, since accumulation rates of paleosols in intra-volcanic horizons vary between  $0.5$ – $1$  mm per annum [Retallack 2021]. Paleosols are not evident between stage 1, 3, and 4 ignimbrites, indicating deposition (and eruptions) was relatively continuous.

Within stage 1, 3, and 4 KVF samples disequilibrium features such as mafic enclaves, rounded and resorbed quartz crystals, resorbed fiamme, or fringing chlorite on fritted alkali feldspar are common (full details of disequilibrium features are in Supplementary Material 1). Mafic enclaves are present throughout KVF ignimbrites and range in size from  $2$  mm– $\leq 2.5$  cm diameter. Enclaves may be streaked out, or circular to subcircular in form (Figures 5E, 6E, H, 7F, and Supplementary Material 1). Replenishment of magma chambers by fresh pulses of basic magma has been cited as the cause of magma chamber tumescence [Tilling 1987; Troll et al. 2004]. We suggest that basic magma repeatedly injected a network of silicic magma reservoirs underneath the developing Kilchrist Caldera inducing tumescence and likely acted as the main eruption trigger [Sparks et al. 1977; Eichelberger 1980; Folch and Martí 1998].

Resurgence of the Eastern Red Hills Centre followed collapse of the Kilchrist Caldera and this is recorded by the emplacement of the Outer Granite and Inner Granite suites of the Eastern Red Hills Centre. We suggest that the Outer Granite ( $\sim 55.89 \pm 0.15$  Ma) developed partially synchronous with late-stage caldera collapse (stages 3 and 4 onwards;  $\sim 55.88 \pm 0.1$  Ma, Figure 16) and was associated with collapsing overburden, remobilisation and shallow intrusion of silicic magma (e.g. Glas Bheinn Mhor, Beinn na Cro, Beinn an Dub-

haich, and Creag Strollamus granites). These intrusions were supplied via a network of magma reservoirs underlying the caldera. Locally, basaltic magma formed resurgent intrusions (e.g. Beinn na Cro and Broadford gabbros). We interpret the Inner Granite of Beinn na Caillich ( $55.7 \pm 0.1$  Ma) as a “true” resurgent phase, completely post-dating caldera collapse. This granite displays no evidence of magma mixing and appears to represent a new, upwelling magmatic body (Figure 16B).

### 8.2 The influence of pre-existing intrusions, regional-scale faults, and extensional tectonics on the location and development of the Kilchrist Caldera

The location, size, shape, and surface expression of the Kilchrist Caldera was probably strongly influenced by several factors. At ~58 Ma a magmatic ‘barrier’ comprising the Cuillin and Western Red Hills centres was in existence 5 km NW of the site where the Kilchrist Caldera (KVF deposits) would become situated (Figures 2, 13 and 14). This barrier prevented northwards magma migration and promoted magma ponding. A contemporaneous regional extensional tectonics regime also ‘overprinted’ both the growth, and collapse of the Kilchrist Caldera. This regime consisted of partially active extensional Jurassic faults, which facilitated sedimentary loading of the Inner Hebrides Basin. One such fault, the Camasunary Fault, was not considered significantly active after the Mid-Jurassic [Morton 1992]. However, in this study we have identified several  $\leq 1.5$  m-wide NNW-trending basic dykes that have been faulted out across the Camasunary Fault in Camasunary Bay (NG 51780 18060; Figure 2). These dykes originally spanned the entire fault trace, and can be matched on either side of it. They intrude footwall Neoproterozoic Applecross Formation west of the fault trace, and hanging wall, Middle Jurassic Great Estuarine Group east of the fault trace. The Camasunary Fault must therefore have been active in an extensional capacity after Paleocene dykes had been intruded and solidified. The Screapadal Fault on Raasay is linked to the Camasunary Fault (Figure 1B) and was also active during/post Paleocene since basic dykes of the regional swarm trend have been deformed across the fault trace [Butler and Hutton 1994]. Such combined evidence at separate localities some 20 km apart, suggests that the Inner Hebrides Basin was still growing throughout KVF eruptions and able to accommodate ponding magma and the growing caldera.

Contemporaneous dyke intrusion, induced by crustal extension linked to North Atlantic Opening was also taking place across the study area. Those basic dykes present within what was to become the inner ring-fault are now largely absent and were probably obscured during caldera growth. To the south of the caldera inner ring-fault, and within the outer margin, numerous NW–NNW-trending dykes also intrude Cambro-Ordovician dolostone (Figure 2). The majority of these dykes crop out east of the Beinn an Dubhaich Granite [Bell and Harris 1986; BGS 2005]. Within the inner ring-fault, sporadic basic dykes of the regional trend also exploited, and intruded, fissures previously intruded by silicic Stage 3 KVF tuff (Figure S10E). Collectively basic dyke intrusion therefore occurred before, during, and after, development of the Kilchrist Caldera.

### 8.3 Magma supply, conduits, pre-existing/contemporaneous folds

We considered the possibility of simple diapiric-type ascent of magma supplying the Kilchrist Caldera but suggest that the data preclude such a hypothesis. Gravity and magnetic surveys have established that granitic bodies are present directly underneath much of the study area [Bott and Tuson 1973; Horsch 1979; Goultly et al. 1996], including beneath Ben Suardal, and critically to the SE of the Kishorn Thrust zone, where numerous composite sills crop out. The geophysical data therefore suggests that the growing Kilchrist caldera was probably fed from a sill-like (not diapiric) magma body (or bodies) situated to the south and southeast of Beinn an Dubhaich. This magma body likely extended east to the region underneath present-day Ben Suardal (Figures 2, 14, 15 and 16) as zircons from the granite inclusions with lobate margins (Figures 10 and 17) that we dated at  $56.45 \pm 0.15$  Ma from a dyke at Ben Suardal indicate a silicic magma body existed here ~300 ka before Stage 3 KVF ignimbrites.

Magma is frequently fed to volcanoes where dykes dominate volcanic plumbing systems [Kendall et al. 2005; Cashman and Sparks 2013; Tibaldi 2015]; however, a growing body of evidence suggests magma is also commonly transported laterally in sills substantial distances from the ultimate site of eruption [Tibaldi 2015; Magee et al. 2016]. The influence of pre-existing regional scale faults on magma transportation via sill complexes has been reported from Western Australia [Magee et al. 2013], the Faroe-Shetland Basin [Schofield et al. 2015], and from the Little Minch Sill Complex [Schofield et al. 2015; Fyfe et al. 2021]. Indeed, Troll et al. [2020] have recently suggested the Long Loch Fault on Rum, NW Scotland, acted as a pulsing magma conduit by opening and closing repeatedly during Paleocene volcano building. Such magmatic exploitation of pre-existing fault planes has experimentally been shown to produce sill-like (oblate ellipsoid) shaped magma reservoirs and indeed caldera collapse is promoted by such shaped magma chambers [Gudmundsson 2008]. We suggest the Kilchrist caldera grew in a similar way and cite the following supporting evidence.

The close proximity of the Kishorn Thrust Fault zone to KVF ignimbrites within the inner ring-fault (Figure 2) and the incorporation of lithic lapilli and blocks of arkosic sandstone (Kishorn Thrust hanging wall block), and Cambro-Ordovician dolostone (Kishorn Thrust footwall block) within KVF ignimbrites suggest the Kishorn Thrust cropped out across the study area before the first eruptions (Figure 13). Scavenging of such components by aggrading PDCs must necessarily have taken place at or near the paleosurface and indicates that the Kishorn Thrust Fault was very close to or covered the paleosurface on which the KVF was deposited (Figure 14). An isolated “megablock” of Archean basement gneiss crops out NW of Creagan Dubh (Figures 2 and 13) and could represent an overthrust section of Kishorn Thrust hanging wall. The fault zone thus represented a convenient, near surface region for migration of magma and other fluids. Indeed, numerous basic dykes and silicic sheets are evident (around NG 6273921648) at the Kishorn Thrust Plane. Elsewhere around Beinn an Dubhaich (Figure 2), highly brecciated dolostone (related to fluid

flow) has also been reported close to the Kishorn Thrust [Holness 1992]. Numerous basic dykes also intrude the country rock in this area, and a 100 m-wide gabbroic sill trends parallel 200 m away from the Kishorn Thrust zone. This sill steps up from Lower Jurassic Ardnish Formation into Pabay Shale and terminates into the silicic core of a composite sill (NG 60420 16850). Substantial bodies of magma were therefore intruded at and in very close proximity to the the Kishorn Thrust Plane in this region and exploited Mesozoic sedimentary layers. Some of this magma fed the composite sills in the study area (Figure 2), exploiting the contact between the Triassic Stornoway Formation and the Lower Jurassic Breakish Formation (between NG 62600 18300 and NG 62870 18450), and the contact between the Lower Jurassic Ardnish (NG 61900 16680–61480 17880) and Pabay Shale formations (NG 59440 16440–60940 16600).

Some early magma-related deformation likely produced the regional Broadford Anticline (Figure 2) as suggested by Walker [1975]. This deformation was probably associated with tumescence of earlier ponding magma reservoirs, and deformed structures include boudinaged basic dykes around Camas Malag, WSW of Beinn an Dubhaich (Figure 2). These dykes have themselves been intruded by apophyses of the later Beinn an Dubhaich Granite.

#### 8.4 PETM-related CO<sub>2</sub> and CH<sub>4</sub> flux resulting from magma intrusion, dissociation, and dehydration during contact metamorphism of country rock

The KVF eruptions detailed in this paper are the first voluminous silicic eruptions recorded within either the NAIP or BPIP that coincide with the onset of the PETM at ~56 Ma. The PETM spanned ~170 kyr [Röhl et al. 2007; Charles et al. 2011; Turner 2018], and was a time when Earth's atmospheric temperatures rose abruptly by ~5–9 °C [Rampino 2013]. This rise was associated with massive injections of <sup>13</sup>C-depleted carbon into the oceans and atmosphere, which is recorded in sedimentary deposits that possess a negative carbon isotope excursion (CIE) [Frieling et al. 2016]. The probable causes of the PETM include gas release associated with volcanism within the North Atlantic Igneous Province [Gutjahr et al. 2017], comet impact [Kent et al. 2003], and contact metamorphism of carbon-rich sedimentary rock which triggered CO<sub>2</sub> release [Storey et al. 2007; Rampino 2013]. During contact metamorphism of carbonate carbon dioxide may also be released into the atmosphere by carbonate dissociation. During this process CaCO<sub>3</sub> rapidly breaks down into CaO and CO<sub>2</sub> [Deegan et al. 2010]. However, dissociation of carbonates (which is characterised by a high δ<sup>13</sup>C signature) is not enough to completely explain the elevated temperature spikes and in particular the CIE seen in the PETM. Degassing of methane (CH<sub>4</sub>) from organic-rich sedimentary rocks resulting from magmatic intrusion has been cited as the most probable mechanism of producing the CIE [Zeebe et al. 2009; Svensen et al. 2010]. Recent modelling suggests that the magnitude of the CIE in the NAIP can only be explained by a large rapid, initial pulse of carbon, followed by ~50 kyr of a carbon injection with a depleted δ<sup>13</sup>C signature [Frieling et al. 2016].

Elevated levels of mercury (Hg) relative to organic carbon within carbon rich sedimentary rock cores are thought to correspond to periods of volcanism during the PETM, with 'pulsed' episodes of such volcanism recently considered to be the PETM trigger in the NAIP [Kender et al. 2021]. However, the onset of the PETM coincided with a mercury low standpoint. This suggests at least one other carbon reservoir must have released significant greenhouse gases to account for the elevated Hg [Kender et al. 2021]. Such a reservoir could have been produced by contact metamorphism, dehydration, and cracking of organic-rich shale [Svensen et al. 2004; Aarnes et al. 2010]. These processes release substantial quantities of CO<sub>2</sub>, and CH<sub>4</sub> into the atmosphere. The release of CH<sub>4</sub> by contact metamorphism of organic-rich shale occurs at temperatures ≤350 °C [Ganino and Arndt 2009]. In our study area highly organic-rich sedimentary rocks are intruded by laterally extensive composite sills, the Kilchrist Hybrid Ring Dyke, basic dykes of the regional swarm, and granite and gabbro which form the Eastern Red Hills Centre (Figures 2 and 3). These organic-rich sedimentary rocks comprise the Lower Jurassic Broadford Beds (<100 m thick) which contains organic-rich fissile mudstone units together with micaceous mudstone units. The Broadford Beds are overlain by the Pabay Shale Formation (maximum of 200 m thickness) a highly organic micaceous mudstone, containing abundant organic particulate matter, mainly terrestrially derived plant fragments, pollen, and spores with relatively low proportions of marine microplankton such as acritarchs and dinoflagellate cysts [Brittain et al. 2010]. In the Hebrides Basin (both in wells and in outcrop) the Pabay Shale [Morton and Hudson 1995] contains kerogen comprising up to 90 % amorphous organic matter, which gives the unit considerable gas potential [Scotchman 2001].

Within the southern extent of the outer marginal zone of the Kilchrist Caldera the Eastern Red Hills Centre granite and gabbro are largely fringed by 31 km<sup>2</sup> of Cambro-Ordovician dolostone—CaMg(CO<sub>3</sub>)<sub>2</sub>—of the Durness Group, which is also cut by numerous basaltic dykes of the regional Paleocene swarm trend (Figure 2). A contact aureole has overprinted the dolostone around the Beinn an Dubhaich Granite [Holness 1992; BGS 2005]. Within this aureole 'isograds' define an outer talc zone (1), tremolite zone (2), diopside zone (3), olivine zone (4), and inner periclase zone (5) (?). During all of these index-mineral producing reactions, CO<sub>2</sub>, H<sub>2</sub>O, or both, were driven off [Holness 1992]. Substantial quantities of brucite (generated by hydration of periclase to brucite at temperatures of ~600 °C) accompanied contact metamorphism. During this conversion process 239 g of CO<sub>2</sub> per kilogram of dolostone is released [Ganino et al. 2013]. The quantity of brucite produced within the Beinn an Dubhaich aureole was substantial since numerous disused brucite-forsterite marble quarries crop out (NG 61560 20060, NG 62130 20070, and NG 57420 21300) south of Loch Kilchrist (Figure 2). Additionally, the working Torrin Quarry (NG 58440 20160) still produces ~20,000 tonnes of brucite and serpentine-rich marble per year [Emeleus and Bell 2005]. Brucite can also be produced at much lower temperatures (~450 °C) if hydrous fluids are present in the system by the reaction: CaMg(CO<sub>3</sub>)<sub>2</sub> (dolomite) + H<sub>2</sub>O → Mg(OH)<sub>2</sub>

(brucite) + CaCO<sub>3</sub> (calcite) + CO<sub>2</sub> [Ganino et al. 2013]. Such fluid was present close to the granite contact in the Beinn an Dubhaich aureole. Here the periclase isograd was affected by substantial volumes of fluid, whilst brecciated dolostone at the extremities of the aureole was also infiltrated by substantial volumes of Si-bearing water [Holness 1992]. Such fluid flow through dolostone would have acted to flush out the CO<sub>2</sub> produced by these reactions [Holness 1992]. Holness [1992] suggests infiltration of aqueous fluid was critical to reaction progress within aureole dolostone, and that the most substantial amounts of fluid infiltration took place within highly brecciated dolostone, nearest the Kishorn Thrust (Figure 2).

The thickness of dolostone country rock within the Beinn an Dubhaich Granite aureole was probably increased substantially during Caledonian compression/Kishorn Thrust development, and a repetition of stratigraphy would be expected [McClay 1987]. Such thickening would substantially increase the volume of dolostone subjected to contact metamorphism by pulses of chemically diverse magmas. Therefore, KVF associated silicic and basic magma injected through magnesium carbonate, and organic-rich shales would have released substantial volumes of CH<sub>4</sub> and CO<sub>2</sub> during the PETM. These intrusions occurred in tandem with the large scale, largely continuous, silicic KVF eruptions whose output of CO<sub>2</sub> and SO<sub>2</sub> into the atmosphere would also have been substantial.

Skye was subaerially exposed during the Paleocene (and therefore throughout KVF eruptions) [Emeleus and Bell 2005]. Gases such as CH<sub>4</sub>, CO<sub>2</sub>, and SO<sub>2</sub> would have been directly introduced into the atmosphere via fractures in cover rock without dilution. However, the gas release scenario in subaqueous settings is more complex, in particular the dilution of CH<sub>4</sub> between sites of subaqueous intrusions/contact metamorphism, dehydration, passage through the water column, and eventual atmospheric incorporation. A recent study in the Beaufort Sea showed that CH<sub>4</sub> levels in shelf bottom waters, generated from Late Pleistocene sediment, and decomposing CH<sub>4</sub> hydrate, had totally different values to surface waters. At or below the 30 m isobath, ancient CH<sub>4</sub> values contributed at most 10 ± 3 % of surface values [Sparrow et al. 2018]. These results suggest oceanic oxidation, and dispersion processes, can strongly limit the emission of ancient CH<sub>4</sub> released into the atmosphere [Sparrow et al. 2018]. Therefore, the quantities of CH<sub>4</sub> released by the emplacement of PETM dated intrusions into organic-rich sedimentary rocks in subaqueous basis [e.g. Vøring and Møre basins, Aarnes et al. 2010] could potentially be reduced by ≤90 % during their passage to the atmosphere [Sparrow et al. 2018]. Given the subaerial association of the Kilchrist Caldera and its magmatic plumbing system, its contribution to the PETM was likely significant.

We suggest silicic and basic magma intruding into >43 km<sup>2</sup> of organic-rich shales and dolostone during KVF eruptions and resurgence may have acted as a PETM trigger point [Kender et al. 2021]. In calculating the CH<sub>4</sub> flux we suggest that 30 % dehydration, cracking, and contact metamorphism of organic-rich shales (Supplementary Table 6) might yield ~88.9 Gt atmospheric flux of CH<sub>4</sub>, a 50 % loss via these processes ~148 Gt, and 80 % loss ~237 Gt. We suggest 30 % contact metamorphism and dissociation of the cumulative dolostone thickness

within the extent of the Kilchrist Caldera (see Supplementary Material 1 for calculations) might yield ~3.9 Gt atmospheric flux of CO<sub>2</sub>, a 50 % loss by these processes ~5.32 Gt, and 80 % loss (in part accounting for footwall thickening resulting from Caledonian compression) ~8.52 Gt. To place this into context, annual anthropogenic CO<sub>2</sub> emissions summed to ~6.3 Gt in the late 20<sup>th</sup> century [Svensen et al. 2004].

## 9 CONCLUSIONS

1. We interpret the KVF as the remnants of a large Paleocene caldera. We record at least four eruption stages (1, 3, and 4 dominantly explosive; 2 dominantly effusive), followed by a subsequent resurgent phase of intrusion.

2. Whilst pre-existing regional structural discontinuities are known to influence caldera morphology and surface expression, we propose deep-rooted, solidified igneous intrusive barriers may act in a similar manner. Prior to the first KVF-forming eruptions, the Cuillin Centre and Western Red Hills Centre acted as a physical barrier to ponding magma, which supplied the growing Kilchrist Caldera, whilst the Kishorn Thrust zone and Mesozoic strata acted as a magma conduit to the growing caldera. Half graben, extensional Mesozoic transfer zones present between the Camasunary Fault and Screapadal faults also provided ponding room for incoming magma to exploit. Throughout Stage 3 KVF-forming eruption stages, vertical NW–NNW fractures generated by regional Paleocene extension punctured the Kishorn Thrust zone magmatic conduit. This resulted in horizontally travelling magma exploiting vertical fractures, and ultimately supplying magma to surface PDCs. Subsequently silicic tuff solidified within fissures. Whilst stage 1, 2, and 4 of KVF eruptions could also have been fissure fed they must necessarily have been linked to tumescence, ring-dyke intrusion and allied faulting, eruptions, and caldera collapse.

3. KVF-forming pyroclastic eruptions were typically silicic in composition; however, a portion of mafic magma was constantly tapped during stages 1, 3, and 4. This melt is evident throughout the matrix of silicic ignimbrites as mafic enclaves which have lobate margins. Magma mixing between chemically diverse magmas was therefore extensive throughout KVF-forming eruptions and subsurface magma chamber(s) were replenished by hotter mafic pulses, which were then injected into cooler bodies of silicic melt. This process probably acted as an eruption trigger as a result of magmatic over pressurisation exceeding country rock confining pressures.

4. Thick repeating sequences of mLT and reverse graded mBr units were deposited throughout stage 1, 3, and 4 KVF eruptions as proximal caldera collapse related ignimbrites. Some Stage 3/4 KVF units were also transported in powerful, high-concentration, silicic PDCs ~6 km to the outside of the northern outer caldera margin where PDCs surmounted topographical highs and deposited ignimbrite on top of granite and gabbro around Belig. The thickness of KVF stage 1, 3, and 4 mLT and mBr units and their typically large block size indicate that the eruptions were frequent, high-energy, pro-

longed, and that multiple collapse events occurred throughout the growth and ultimate collapse of the Kilchrist caldera.

5. KVF-forming eruptions took place precisely on the PETM at  $56.15 \pm 0.19$  Ma where barrier-induced magmatic ponding promoted contact metamorphism and dissociation of large volumes of Cambro-Ordovician dolostone, and contact metamorphism, dehydration, and cracking of organic-rich Lower Jurassic sedimentary rocks. Very substantial amounts of  $\text{CO}_2$  and  $\text{CH}_4$  were driven off as a result, which we suggest would have had a profound effect on the Paleocene atmosphere and was a significant contributor/tipping point to the PETM, in both the BPIP, and much larger NAIP.

## AUTHOR CONTRIBUTIONS

SD conceptualised the study, wrote the majority of the manuscript and produced most of the figures, as well as conducting fieldwork, sampling, mapping and subsequent geochemical analysis as part of his PhD studies. DB conducted fieldwork, conceptualised and created eruption diagrams and some other figures, and wrote parts of the manuscript as well as editing, and supervised the project. AB conducted fieldwork and supervised geochemical analysis and EMP studies. PK and DT assisted with fieldwork including logging. CB conducted fieldwork. IM and KG assisted with sampling for U-Pb dating, subsequent methodology and analysis, and some manuscript and figure editing.

## ACKNOWLEDGEMENTS

This paper is dedicated to the memory of Barbara Smith of Birkbeck College a dear friend who loved Skye. Brin Roberts and Henry Emeleus are also remembered and recognised for invaluable guidance, patience, and endless good humour. Rebecca and Paul Smith are thanked for accommodation at Torrin. We are grateful for funding assistance from the Central Research Fund, University of London, and NERC Isotope Geosciences Facilities Steering Committee grant IP-1207-1110 (“Ignimbrite magmatism in the British Palaeogene Igneous Province: assessing the frequency of large-volume silicic eruptions.”, P. I. - Goodenough, K. M.). We would like to thank two anonymous reviewers for their helpful suggestions and support, which improved the manuscript, and editorial support from Volcanica.

## DATA AVAILABILITY

The data analysed in this paper are available in [Supplementary Material 1](#).

## COPYRIGHT NOTICE

© The Author(s) 2022. This article is distributed under the terms of the [Creative Commons Attribution 4.0 International License](#), which permits unrestricted use, distribution, and reproduction in any medium, provided you give appropriate credit to the original author(s) and the source, provide a link to the Creative Commons license, and indicate if changes were made.

## REFERENCES

- Aarnes, I., H. Svensen, J. A. Connolly, and Y. Y. Podladchikov (2010). “How contact metamorphism can trigger global climate changes: Modeling gas generation around igneous sills in sedimentary basins”. *Geochimica et Cosmochimica Acta* 74(24), pages 7179–7195. ISSN: 0016-7037. DOI: [10.1016/j.gca.2010.09.011](#).
- Andrews, G. D. M. and M. J. Branney (2011). “Emplacement and rheomorphic deformation of a large, lava-like rhyolitic ignimbrite: Grey’s Landing, southern Idaho”. *Geological Society of America Bulletin* 123(3–4), pages 725–743. ISSN: 1943-2674. DOI: [10.1130/b30167.1](#).
- Archer, S. G., R. J. Steel, D. Mellere, S. Blackwood, and B. Cullen (2019). “Response of Middle Jurassic shallow-marine environments to syn-depositional block tilting: Isles of Skye and Raasay, NW Scotland”. *Scottish Journal of Geology* 55(1), pages 35–68. ISSN: 2041-4951. DOI: [10.1144/sjg2018-014](#).
- Bailey, E. (1955). “Moine tectonics and metamorphism in Skye”. *Transactions of the Edinburgh Geological Society* 16(2), pages 93–166. DOI: [10.1144/transed.16.2.93](#).
- Barber, A. (1965). “The history of the Moine Thrust Zone, Lochcarron and Lochalsh, Scotland”. *Proceedings of the Geologists’ Association* 76(3), pages 215–242. DOI: [10.1016/s0016-7878\(65\)80026-8](#).
- Bell, B. R. and J. W. Harris (1986). *An excursion guide to the geology of the Isle of Skye*. Geological Society of Glasgow. ISBN: 0902892088.
- Bell, B. R. (1984). “The basic lavas of the Eastern Red Hills district, Isle of Skye”. *Scottish Journal of Geology* 20(1), pages 73–86. DOI: [10.1144/sjg20010073](#).
- (1985). “The pyroclastic rocks and rhyolitic lavas of the Eastern Red Hills district, Isle of Skye”. *Scottish Journal of Geology* 21(1), pages 57–70. ISSN: 2041-4951. DOI: [10.1144/sjg21010057](#).
- Bell, B. R. and I. T. Williamson (1994). “Picritic basalts from the Palaeocene lava field of west-central Skye, Scotland: evidence for parental magma compositions”. *Mineralogical Magazine* 58(392), pages 347–356. DOI: [10.1180/minmag.1994.058.392.01](#).
- Bell, J. D. (1966). “XIII.—Granites and Associated Rocks of the Eastern Part of the Western Redhills Complex, Isle of Skye”. *Transactions of the Royal Society of Edinburgh* 66(13), pages 307–343. ISSN: 2053-5945. DOI: [10.1017/s0080456800023632](#).
- (1976). “The Tertiary intrusive complex on the Isle of Skye”. *Proceedings of the Geologists’ Association* 87(3), pages 247–271. DOI: [10.1016/s0016-7878\(76\)80001-6](#).
- Bierwith, P. N. (1982). “Experimental welding of volcanic ash”. Master’s thesis. Monash University.
- Blair, T. C. and J. G. McPherson (1998). “Recent debris-flow processes and resultant form and facies of the Dolomite alluvial fan, Owens Valley, California”. *Journal of Sedimentary Research* 68(5), pages 800–818. ISSN: 1527-1404. DOI: [10.2110/jsr.68.800](#).
- Bott, M. H. P. and J. Tuson (1973). “Deep Structure beneath the Tertiary Volcanic Regions of Skye, Mull and Ardnurchan, North-west Scotland”. *Nature Physical Science*

- 242(121), pages 114–116. ISSN: 2058-1106. DOI: [10.1038/physci242114a0](https://doi.org/10.1038/physci242114a0).
- Branney, M. J. and P. Kokelaar (1992). “A reappraisal of ignimbrite emplacement: progressive aggradation and changes from particulate to non-particulate flow during emplacement of high-grade ignimbrite”. *Bulletin of Volcanology* 54(6), pages 504–520. ISSN: 1432-0819. DOI: [10.1007/bf00301396](https://doi.org/10.1007/bf00301396).
- (1994). “Volcanotectonic faulting, soft-state deformation, and rheomorphism of tuffs during development of a piece-meal caldera, English Lake District”. *Geological Society of America Bulletin* 106(4), pages 507–530. DOI: [10.1130/0016-7606\(1994\)106<0507:vfssda>2.3.co;2](https://doi.org/10.1130/0016-7606(1994)106<0507:vfssda>2.3.co;2).
- (2002). “Pyroclastic Density Currents and the Sedimentation of Ignimbrites”. 27(1). DOI: [10.1144/gsl.mem.2003.027](https://doi.org/10.1144/gsl.mem.2003.027).
- British Geological Survey (BGS) (2005). *Skye Central Complex, Scotland, Bedrock*. 1:25000 British Geology Series. Keyworth, Nottingham, British Geological Survey.
- Brittain, J. M., K. T. Higgs, and J. B. Riding (2010). “The palynology of the Pabay Shale Formation (Lower Jurassic) of SW Raasay, northern Scotland”. *Scottish Journal of Geology* 46(1), pages 67–75. ISSN: 2041-4951. DOI: [10.1144/0036-9276/01-391](https://doi.org/10.1144/0036-9276/01-391).
- Brown, D. J. and B. R. Bell (2007). “How do you grade peperites?” *Journal of Volcanology and Geothermal Research* 159(4), pages 409–420. ISSN: 0377-0273. DOI: [10.1016/j.jvolgeores.2006.08.008](https://doi.org/10.1016/j.jvolgeores.2006.08.008).
- (2013). “The emplacement of a large, chemically zoned, rheomorphic, lava-like ignimbrite: the Sgurr of Eigg Pitchstone, NW Scotland”. *Journal of the Geological Society* 170(5), pages 753–767. ISSN: 2041-479X. DOI: [10.1144/jgs2012-147](https://doi.org/10.1144/jgs2012-147).
- Brown, D. J., E. P. Holohan, and B. R. Bell (2009). “Sedimentary and volcano-tectonic processes in the British Paleocene Igneous Province: a review”. *Geological Magazine* 146(3), pages 326–352. ISSN: 1469-5081. DOI: [10.1017/s0016756809006232](https://doi.org/10.1017/s0016756809006232).
- Brown, R. J., M. J. Branney, C. Maher, and P. Davila-Harris (2010). “Origin of accretionary lapilli within ground-hugging density currents: Evidence from pyroclastic couplets on Tenerife”. *Geological Society of America Bulletin* 122(1-2), pages 305–320. DOI: [10.1130/b26449.1](https://doi.org/10.1130/b26449.1).
- Butler, R. W. H. and D. H. W. Hutton (1994). “Basin structure and Tertiary magmatism on Skye, NW Scotland”. *Journal of the Geological Society* 151(6), pages 931–944. ISSN: 2041-479X. DOI: [10.1144/gsjgs.151.6.0931](https://doi.org/10.1144/gsjgs.151.6.0931).
- Cashman, K. V. and R. S. J. Sparks (2013). “How volcanoes work: A 25 year perspective”. *Geological Society of America Bulletin* 125(5-6), pages 664–690. DOI: [10.1130/b30720.1](https://doi.org/10.1130/b30720.1).
- Chambers, L. M. and M. S. Pringle (2001). “Age and duration of activity at the Isle of Mull Tertiary igneous centre, Scotland, and confirmation of the existence of subchrons during Anomaly 26r”. *Earth and Planetary Science Letters* 193(3-4), pages 333–345. DOI: [10.1016/s0012-821x\(01\)00499-x](https://doi.org/10.1016/s0012-821x(01)00499-x).
- Chambers, L. M., M. S. Pringle, and R. R. Parrish (2005). “Rapid formation of the Small Isles Tertiary centre constrained by precise  $^{40}\text{Ar}/^{39}\text{Ar}$  and U–Pb ages”. *Lithos* 79(3-4), pages 367–384. DOI: [10.1016/j.lithos.2004.09.008](https://doi.org/10.1016/j.lithos.2004.09.008).
- Charles, A. J., D. J. Condon, I. C. Harding, H. Pälke, J. E. A. Marshall, Y. Cui, L. Kump, and I. W. Croudace (2011). “Constraints on the numerical age of the Paleocene-Eocene boundary”. *Geochemistry, Geophysics, Geosystems* 12(6). ISSN: 1525-2027. DOI: [10.1029/2010gc003426](https://doi.org/10.1029/2010gc003426).
- Clough, C. T., H. B. Maufe, and E. B. Bailey (1909). “The Cauldron-Subsidence of Glen Coe, and the Associated Igneous Phenomena”. *Quarterly Journal of the Geological Society* 65(1-4), pages 611–678. DOI: [10.1144/gsl.jgs.1909.065.01-04.35](https://doi.org/10.1144/gsl.jgs.1909.065.01-04.35).
- Cole, J., D. Milner, and K. Spinks (2005). “Calderas and caldera structures: a review”. *Earth-Science Reviews* 69(1–2), pages 1–26. ISSN: 0012-8252. DOI: [10.1016/j.earscirev.2004.06.004](https://doi.org/10.1016/j.earscirev.2004.06.004).
- Costa, A., J. Gottsmann, O. Melnik, and R. Sparks (2011). “A stress-controlled mechanism for the intensity of very large magnitude explosive eruptions”. *Earth and Planetary Science Letters* 310(1–2), pages 161–166. ISSN: 0012-821X. DOI: [10.1016/j.epsl.2011.07.024](https://doi.org/10.1016/j.epsl.2011.07.024).
- Coward, M. and J. Whalley (1979). “Texture and fabric studies across the Kishorn Nappe, near Kyle of Lochalsh, Western Scotland”. *Journal of Structural Geology* 1(4), pages 259–273. DOI: [10.1016/0191-8141\(79\)90001-4](https://doi.org/10.1016/0191-8141(79)90001-4).
- Deegan, F. M., V. R. Troll, C. Freda, V. Misiti, J. P. Chadwick, C. L. McLeod, and J. P. Davidson (2010). “Magma–Carbonate Interaction Processes and Associated CO<sub>2</sub> Release at Merapi Volcano, Indonesia: Insights from Experimental Petrology”. *Journal of Petrology* 51(5), pages 1027–1051. ISSN: 0022-3530. DOI: [10.1093/petrology/egq010](https://doi.org/10.1093/petrology/egq010).
- Drake, S. M. (2015). “Silicic pyroclastic density current deposits on the Isle of Skye, NW Scotland and implications for the volcanic evolution of the Palaeogene Skye Central Complex”. PhD thesis. University of London.
- Drake, S. M. and A. D. Beard (2012). “Silicic pyroclastic deposits at the base of the Paleogene Skye Lava Field: Evidence from An Carnach, Strathaird Peninsula”. *Scottish Journal of Geology* 48(2), pages 133–141. ISSN: 2041-4951. DOI: [10.1144/sjg2012-445](https://doi.org/10.1144/sjg2012-445).
- Drake, S. M., A. D. Beard, A. P. Jones, D. J. Brown, A. D. Fortes, I. L. Millar, A. Carter, J. Baca, and H. Downes (2017). “Discovery of a meteoritic ejecta layer containing unmelted impactor fragments at the base of Paleocene lavas, Isle of Skye, Scotland”. *Geology* 46(2), pages 171–174. ISSN: 0091-7613. DOI: [10.1130/g39452.1](https://doi.org/10.1130/g39452.1).
- Eichelberger, J. C. (1980). “Vesiculation of mafic magma during replenishment of silicic magma reservoirs”. *Nature* 288(5790), pages 446–450. ISSN: 1476-4687. DOI: [10.1038/288446a0](https://doi.org/10.1038/288446a0).
- Emeleus, C. H. and B. R. Bell (2005). *The Palaeogene volcanic districts of Scotland*. Volume 3. British Geological Survey Nottingham.
- England, R. W. (1988). “The early Tertiary stress regime in NW Britain: evidence from the patterns of volcanic activity”. *Geological Society, London, Special Publications*

- 39(1), pages 381–389. DOI: [10.1144/gsl.sp.1988.039.01.33](https://doi.org/10.1144/gsl.sp.1988.039.01.33).
- Ferré, E. C., O. Galland, D. Montanari, and T. J. Kalakay (2012). “Granite magma migration and emplacement along thrusts”. *International Journal of Earth Sciences* 101(7), pages 1673–1688. ISSN: 1437-3262. DOI: [10.1007/s00531-012-0747-6](https://doi.org/10.1007/s00531-012-0747-6).
- Folch, A. and J. Martí (1998). “The generation of overpressure in felsic magma chambers by replenishment”. *Earth and Planetary Science Letters* 163(1-4), pages 301–314. DOI: [10.1016/S0012-821X\(98\)00196-4](https://doi.org/10.1016/S0012-821X(98)00196-4).
- Freundt, A. (1998). “The formation of high-grade ignimbrites, I: Experiments on high- and low-concentration transport systems containing sticky particles”. *Bulletin of Volcanology* 59(6), pages 414–435. ISSN: 1432-0819. DOI: [10.1007/s004450050201](https://doi.org/10.1007/s004450050201).
- Frieling, J., H. H. Svensen, S. Planke, M. J. Cramwinckel, H. Selnes, and A. Sluijs (2016). “Thermogenic methane release as a cause for the long duration of the PETM”. *Proceedings of the National Academy of Sciences* 113(43), pages 12059–12064. ISSN: 1091-6490. DOI: [10.1073/pnas.1603348113](https://doi.org/10.1073/pnas.1603348113).
- Fyfe, L.-J. C., N. Schofield, S. P. Holford, D. A. Jerram, and A. Hartley (2021). “Emplacement of the Little Minch Sill Complex, Sea of Hebrides Basin, NW Scotland”. *Journal of the Geological Society* 178(3). ISSN: 2041-479X. DOI: [10.1144/jgs2020-177](https://doi.org/10.1144/jgs2020-177).
- Ganino, C. and N. T. Arndt (2009). “Climate changes caused by degassing of sediments during the emplacement of large igneous provinces”. *Geology* 37(4), pages 323–326. ISSN: 0091-7613. DOI: [10.1130/G25325a.1](https://doi.org/10.1130/G25325a.1).
- Ganino, C., N. T. Arndt, C. Chauvel, A. Jean, and C. Athurion (2013). “Melting of carbonate wall rocks and formation of the heterogeneous aureole of the Panzhihua intrusion, China”. *Geoscience Frontiers* 4(5), pages 535–546. ISSN: 1674-9871. DOI: [10.1016/j.gsf.2013.01.012](https://doi.org/10.1016/j.gsf.2013.01.012).
- Gooday, R. J., D. J. Brown, K. M. Goodenough, and A. C. Kerr (2018). “A proximal record of caldera-forming eruptions: the stratigraphy, eruptive history and collapse of the Palaeogene Arran caldera, western Scotland”. *Bulletin of Volcanology* 80(9). DOI: [10.1007/s00445-018-1243-z](https://doi.org/10.1007/s00445-018-1243-z).
- Goultly, N. R., C. E. Darton, A. E. Dent, and K. R. Richardson (1996). “Geophysical investigation of the Beinn an Dubhaich Granite, Skye”. *Geological Magazine* 133(2), pages 171–176. ISSN: 1469-5081. DOI: [10.1017/S001675680008682](https://doi.org/10.1017/S001675680008682).
- Gudmundsson, A. (2008). “Chapter 8 Magma-Chamber Geometry, Fluid Transport, Local Stresses and Rock Behaviour During Collapse Caldera Formation”. *Caldera Volcanism: Analysis, Modelling and Response*. Edited by J. Gottsmann and J. Martí. Elsevier, pages 313–349. DOI: [10.1016/S1871-644X\(07\)00008-3](https://doi.org/10.1016/S1871-644X(07)00008-3).
- Gutjahr, M., A. Ridgwell, P. F. Sexton, E. Anagnostou, P. N. Pearson, H. Pälike, R. D. Norris, E. Thomas, and G. L. Foster (2017). “Very large release of mostly volcanic carbon during the Palaeocene–Eocene Thermal Maximum”. *Nature* 548(7669), pages 573–577. ISSN: 1476-4687. DOI: [10.1038/nature23646](https://doi.org/10.1038/nature23646).
- Hamilton, M. A., D. G. Pearson, R. N. Thompson, S. P. Kelley, and C. H. Emeleus (1998). “Rapid eruption of Skye lavas inferred from precise U–Pb and Ar–Ar dating of the Rum and Cuillin plutonic complexes”. *Nature* 394(6690), pages 260–263. ISSN: 1476-4687. DOI: [10.1038/28361](https://doi.org/10.1038/28361).
- Harker, A. and C. T. Clough (1904). “The Tertiary igneous rocks of Skye”. DOI: [10.5962/bhl.title.115397](https://doi.org/10.5962/bhl.title.115397).
- Hoersch, A. L. (1979). “General structure of the Skye Tertiary igneous complex and detailed structure of the Beinn an Dubhaich Granite from magnetic evidence”. *Scottish Journal of Geology* 15(3), pages 231–245. DOI: [10.1144/SJG15030231](https://doi.org/10.1144/SJG15030231).
- Holness, M. B. (1992). “Metamorphism and Fluid Infiltration of the Calc-silicate Aureole of the Beinn an Dubhaich Granite, Skye”. *Journal of Petrology* 33(6), pages 1261–1293. DOI: [10.1093/ptrology/33.6.1261](https://doi.org/10.1093/ptrology/33.6.1261).
- Holohan, E. P., V. R. Troll, M. Errington, C. H. Donaldson, G. R. Nicoll, and C. H. Emeleus (2009). “The Southern Mountains Zone, Isle of Rum, Scotland: volcanic and sedimentary processes upon an uplifted and subsided magma chamber roof”. *Geological Magazine* 146(3), pages 400–418. ISSN: 1469-5081. DOI: [10.1017/S0016756808005876](https://doi.org/10.1017/S0016756808005876).
- Holroyd, J. D. (1994). “The structure and stratigraphy of the Suardal area, Isle of Skye, north-west Scotland: an investigation of Tertiary deformation in the Skye Volcanic Complex”. PhD thesis. University of Manchester.
- Jordan, N. J., S. G. Rotolo, R. Williams, F. Speranza, W. C. McIntosh, M. J. Branney, and S. Scaillet (2018). “Explosive eruptive history of Pantelleria, Italy: Repeated caldera collapse and ignimbrite emplacement at a peralkaline volcano”. *Journal of Volcanology and Geothermal Research* 349, pages 47–73. ISSN: 0377-0273. DOI: [10.1016/j.jvolgeores.2017.09.013](https://doi.org/10.1016/j.jvolgeores.2017.09.013).
- Kendall, J.-M., G. W. Stuart, C. J. Ebinger, I. D. Bastow, and D. Keir (2005). “Magma-assisted rifting in Ethiopia”. *Nature* 433(7022), pages 146–148. DOI: [10.1038/nature03161](https://doi.org/10.1038/nature03161).
- Kender, S., K. Bogus, G. K. Pedersen, K. Dybkjær, T. A. Mather, E. Mariani, A. Ridgwell, J. B. Riding, T. Wagner, S. P. Hesselbo, and M. J. Leng (2021). “Paleocene/Eocene carbon feedbacks triggered by volcanic activity”. *Nature Communications* 12(1). ISSN: 2041-1723. DOI: [10.1038/s41467-021-25536-0](https://doi.org/10.1038/s41467-021-25536-0).
- Kent, D., B. Cramer, L. Lanci, D. Wang, J. Wright, and R. V. der Voo (2003). “A case for a comet impact trigger for the Paleocene/Eocene thermal maximum and carbon isotope excursion”. *Earth and Planetary Science Letters* 211(1-2), pages 13–26. DOI: [10.1016/S0012-821X\(03\)00188-2](https://doi.org/10.1016/S0012-821X(03)00188-2).
- Magée, C., C. A.-L. Jackson, and N. Schofield (2013). “The influence of normal fault geometry on igneous sill emplacement and morphology”. *Geology* 41(4), pages 407–410. DOI: [10.1130/G33824.1](https://doi.org/10.1130/G33824.1).
- Magée, C., J. D. Muirhead, A. Karvelas, S. P. Holford, C. A.-L. Jackson, I. D. Bastow, N. Schofield, C. T. Stevenson, C. McLean, W. McCarthy, and O. Shtukert (2016). “Lateral magma flow in mafic sill complexes”. *Geosphere* 12(3), pages 809–841. ISSN: 1553-040X. DOI: [10.1130/GES01256.1](https://doi.org/10.1130/GES01256.1).
- McClay, K. R. (1987). *The mapping of geological structures*. Open University Press.

- Moore, I. A. N. and P. Kokelaar (1997). “Tectonic influences in piecemeal caldera collapse at Glencoe Volcano, Scotland”. *Journal of the Geological Society* 154(5), pages 765–768. ISSN: 2041-479X. DOI: [10.1144/gsjgs.154.5.0765](https://doi.org/10.1144/gsjgs.154.5.0765).
- Morton, N. (1992). “Dynamic stratigraphy of the Triassic and Jurassic of the Hebrides Basin, NW Scotland”. *Geological Society, London, Special Publications* 62(1), pages 97–110. ISSN: 2041-4927. DOI: [10.1144/gsl.sp.1992.062.01.10](https://doi.org/10.1144/gsl.sp.1992.062.01.10).
- Morton, N. and J. D. Hudson (1995). “Field guide to the Jurassic of Raasay and Skye, Inner Hebrides, NW Scotland”. *Field Geology of the British Jurassic*. Edited by P. D. Taylor. Geological Society London, pages 209–280. ISBN: 1-897799-41-1.
- Nicholson, R. (1985). “The intrusion and deformation of Tertiary minor sheet intrusions, west Suardal, Isle of Skye, Scotland”. *Geological Journal* 20(1), pages 53–72. DOI: [10.1002/gj.3350200106](https://doi.org/10.1002/gj.3350200106).
- Peach, B. N., J. Horne, H. B. Woodward, C. T. Clough, G. Barrow, J. S. Flett, A. Harker, F. L. Kitchin, J. J. H. Teall, and C. B. Wedd (1910). “The geology of Glenelg, Lochalsh and south-east part of Skye (Explanation of one-inch map 71)”. *Memoirs of the Geological Survey of Great Britain*.
- Potts, G. J. (1993). “The origin of recumbent fold nappes: The Localsh Fold as the main example”. PhD thesis. University of Leeds.
- Rampino, M. R. (2013). “Peraluminous igneous rocks as an indicator of thermogenic methane release from the North Atlantic Volcanic Province at the time of the Paleocene–Eocene Thermal Maximum (PETM)”. *Bulletin of Volcanology* 75(1). ISSN: 1432-0819. DOI: [10.1007/s00445-012-0678-x](https://doi.org/10.1007/s00445-012-0678-x).
- Rateau, R., N. Schofield, and M. Smith (2013). “The potential role of igneous intrusions on hydrocarbon migration, West of Shetland”. *Petroleum Geoscience* 19(3), pages 259–272. ISSN: 2041-496X. DOI: [10.1144/petgeo2012-035](https://doi.org/10.1144/petgeo2012-035).
- Ray, P. S. (1962). “A Note on Some Acid Breccias in the Kilchrist Vent, Skye”. *Geological Magazine* 99(5), pages 420–426. ISSN: 1469-5081. DOI: [10.1017/s0016756800059689](https://doi.org/10.1017/s0016756800059689).
- (1972). “A Rhyolitic Injection-Breccia in Tuff near Allt Slapin, Strath, Skye, Scotland”. *Geological Magazine* 109(5), pages 427–434. ISSN: 1469-5081. DOI: [10.1017/s0016756800039819](https://doi.org/10.1017/s0016756800039819).
- Retallack, G. J. (1988). “Field recognition of paleosols”. *Paleosols and Weathering Through Geologic Time: Principles and Applications*, pages 1–20. ISSN: 0072-1077. DOI: [10.1130/spe216-p1](https://doi.org/10.1130/spe216-p1).
- (2021). “Soil, Soil Processes, and Paleosols”. *Encyclopedia of Geology*, pages 690–707. DOI: [10.1016/b978-0-12-409548-9.12537-0](https://doi.org/10.1016/b978-0-12-409548-9.12537-0).
- Richey, J. E. (1932). “II.— Tertiary Ring Structures in Britain”. *Transactions of the Geological Society of Glasgow* 19(1), pages 42–140. ISSN: 2052-9422. DOI: [10.1144/transglas.19.1.42](https://doi.org/10.1144/transglas.19.1.42).
- Robert, G., G. D. Andrews, J. Ye, and A. G. Whittington (2013). “Rheological controls on the emplacement of extremely high-grade ignimbrites”. *Geology* 41(9), pages 1031–1034. ISSN: 0091-7613. DOI: [10.1130/g34519.1](https://doi.org/10.1130/g34519.1).
- Roberts, A. M. and R. E. Holdsworth (1999). “Linking onshore and offshore structures: Mesozoic extension in the Scottish Highlands”. *Journal of the Geological Society* 156(6), pages 1061–1064. DOI: [10.1144/gsjgs.156.6.1061](https://doi.org/10.1144/gsjgs.156.6.1061).
- Röhl, U., T. Westerhold, T. J. Bralower, and J. C. Zachos (2007). “On the duration of the Paleocene-Eocene thermal maximum (PETM)”. *Geochemistry, Geophysics, Geosystems* 8(12). ISSN: 1525-2027. DOI: [10.1029/2007gc001784](https://doi.org/10.1029/2007gc001784).
- Russell, J., D. Giordano, and D. Dingwell (2003). “High-temperature limits on viscosity of non-Arrhenian silicate melts”. *American Mineralogist* 88(8–9), pages 1390–1394. ISSN: 0003-004X. DOI: [10.2138/am-2003-8-924](https://doi.org/10.2138/am-2003-8-924).
- Saunders, A. D., J. G. Fitton, A. C. Kerr, M. J. Norry, R. W. Kent, J. J. Mahoney, and M. F. Coffin (1997). “The north Atlantic igneous province”. *Large igneous provinces*. Edited by J. J. Mahoney and M. F. Coffin. Volume 100. AGU American Geophysical Union, pages 45–94.
- Schmitz, M. D. and B. Schoene (2007). “Derivation of isotope ratios, errors, and error correlations for U-Pb geochronology using 205Pb-235U-(233U)-spiked isotope dilution thermal ionization mass spectrometric data”. *Geochemistry, Geophysics, Geosystems* 8(8). ISSN: 1525-2027. DOI: [10.1029/2006gc001492](https://doi.org/10.1029/2006gc001492).
- Schofield, N., S. Holford, J. Millett, D. Brown, D. Jolley, S. R. Passey, D. Muirhead, C. Grove, C. Magee, J. Murray, M. Hole, C. A.-L. Jackson, and C. Stevenson (2015). “Regional magma plumbing and emplacement mechanisms of the Faroe-Shetland Sill Complex: implications for magma transport and petroleum systems within sedimentary basins”. *Basin Research* 29(1), pages 41–63. ISSN: 0950-091X. DOI: [10.1111/bre.12164](https://doi.org/10.1111/bre.12164).
- Scotchman, I. C. (2001). “Petroleum geochemistry of the Lower and Middle Jurassic in Atlantic margin basins of Ireland and the UK”. *Geological Society, London, Special Publications* 188(1), pages 31–60. ISSN: 2041-4927. DOI: [10.1144/gsl.sp.2001.188.01.03](https://doi.org/10.1144/gsl.sp.2001.188.01.03).
- Smith, N. J. and B. P. Kokelaar (2013). “Proximal record of the 273 ka Poris caldera-forming eruption, Las Cañadas, Tenerife”. *Bulletin of Volcanology* 75(11). ISSN: 1432-0819. DOI: [10.1007/s00445-013-0768-4](https://doi.org/10.1007/s00445-013-0768-4).
- Smith, S. (1958). “Some aspects of the igneous and metamorphic geology of Central Skye”. PhD thesis. University of Edinburgh.
- Sparks, S. R. J., H. Sigurdsson, and L. Wilson (1977). “Magma mixing: a mechanism for triggering acid explosive eruptions”. *Nature* 267(5609), pages 315–318. ISSN: 1476-4687. DOI: [10.1038/267315a0](https://doi.org/10.1038/267315a0).
- Sparrow, K. J., J. D. Kessler, J. R. Southon, F. Garcia-Tigeros, K. M. Schreiner, C. D. Ruppel, J. B. Miller, S. J. Lehman, and X. Xu (2018). “Limited contribution of ancient methane to surface waters of the U.S. Beaufort Sea shelf”. *Science Advances* 4(1). ISSN: 2375-2548. DOI: [10.1126/sciadv.aao4842](https://doi.org/10.1126/sciadv.aao4842).
- Storey, M., R. A. Duncan, and C. Tegner (2007). “Timing and duration of volcanism in the North Atlantic Igneous Province: Implications for geodynamics and links to the Iceland hotspot”. *Chemical Geology* 241(3–4), pages 264–281. ISSN: 0009-2541. DOI: [10.1016/j.chemgeo.2007.01.016](https://doi.org/10.1016/j.chemgeo.2007.01.016).

- Svensen, H., S. Planke, and F. Corfu (2010). "Zircon dating ties NE Atlantic sill emplacement to initial Eocene global warming". *Journal of the Geological Society* 167(3), pages 433–436. ISSN: 2041-479X. DOI: [10.1144/0016-76492009-125](https://doi.org/10.1144/0016-76492009-125).
- Svensen, H., S. Planke, A. Malthé-Sørensen, B. Jamtveit, R. Myklebust, T. Rasmussen Eidem, and S. S. Rey (2004). "Release of methane from a volcanic basin as a mechanism for initial Eocene global warming". *Nature* 429(6991), pages 542–545. ISSN: 1476-4687. DOI: [10.1038/nature02566](https://doi.org/10.1038/nature02566).
- Thompson, R. N., A. P. Dickin, I. L. Gibson, and M. A. Morrison (1982). "Elemental fingerprints of isotopic contamination of hebridean Palaeocene mantle-derived magmas by archaean sial". *Contributions to Mineralogy and Petrology* 79(2), pages 159–168. DOI: [10.1007/bf01132885](https://doi.org/10.1007/bf01132885).
- Tibaldi, A. (2015). "Structure of volcano plumbing systems: A review of multi-parametric effects". *Journal of Volcanology and Geothermal Research* 298, pages 85–135. DOI: [10.1016/j.jvolgeores.2015.03.023](https://doi.org/10.1016/j.jvolgeores.2015.03.023).
- Tilling, R. I. (1987). "Fluctuations in surface height of active lava lakes during 1972-1974 Mauna Ulu Eruption, Kilauea Volcano, Hawaii". *Journal of Geophysical Research: Solid Earth* 92(B13), pages 13721–13730. ISSN: 0148-0227. DOI: [10.1029/jb092ib13p13721](https://doi.org/10.1029/jb092ib13p13721).
- Troll, V. R., T. Mattsson, B. G. J. Upton, C. H. Emeleus, C. H. Donaldson, R. Meyer, F. Weis, B. Dahrén, and T. H. Heimdal (2020). "Fault-Controlled Magma Ascent Recorded in the Central Series of the Rum Layered Intrusion, NW Scotland". *Journal of Petrology* 61(10). ISSN: 1460-2415. DOI: [10.1093/petrology/egaa093](https://doi.org/10.1093/petrology/egaa093).
- Troll, V. R., C. H. Donaldson, and C. H. Emeleus (2004). "Pre-eruptive magma mixing in ash-flow deposits of the Tertiary Rum Igneous Centre, Scotland". *Contributions to Mineralogy and Petrology* 147(6), pages 722–739. ISSN: 1432-0967. DOI: [10.1007/s00410-004-0584-0](https://doi.org/10.1007/s00410-004-0584-0).
- Troll, V. R., C. H. Emeleus, and C. H. Donaldson (2000). "Caldera formation in the Rum Central Igneous Complex, Scotland". *Bulletin of Volcanology* 62(4–5), pages 301–317. ISSN: 1432-0819. DOI: [10.1007/s004450000099](https://doi.org/10.1007/s004450000099).
- Turner, S. K. (2018). "Constraints on the onset duration of the Paleocene–Eocene Thermal Maximum". *Philosophical Transactions of the Royal Society A: Mathematical, Physical and Engineering Sciences* 376(2130), page 20170082. ISSN: 1471-2962. DOI: [10.1098/rsta.2017.0082](https://doi.org/10.1098/rsta.2017.0082).
- Van Eaton, A. R., L. G. Mastin, M. Herzog, H. F. Schwaiger, D. J. Schneider, K. L. Wallace, and A. B. Clarke (2015). "Hail formation triggers rapid ash aggregation in volcanic plumes". *Nature Communications* 6(1). ISSN: 2041-1723. DOI: [10.1038/ncomms8860](https://doi.org/10.1038/ncomms8860).
- Walker, G. P. L. (1975). "A new concept of the evolution of the British Tertiary intrusive centres". *Journal of the Geological Society* 131(2), pages 121–141. DOI: [10.1144/gsjgs.131.2.0121](https://doi.org/10.1144/gsjgs.131.2.0121).
- (1983). "Ignimbrite types and ignimbrite problems". *Journal of Volcanology and Geothermal Research* 17(1-4), pages 65–88. DOI: [10.1016/0377-0273\(83\)90062-8](https://doi.org/10.1016/0377-0273(83)90062-8).
- White, J. D. L., J. McPhie, and I. Skilling (2000). "Peperite: a useful genetic term". *Bulletin of Volcanology* 62(1), pages 65–66. ISSN: 1432-0819. DOI: [10.1007/s004450050293](https://doi.org/10.1007/s004450050293).
- Williamson, I. T. and B. R. Bell (1994). "The Palaeocene lava field of west-central Skye, Scotland: Stratigraphy, palaeogeography and structure". *Transactions of the Royal Society of Edinburgh: Earth Sciences* 85(1), pages 39–75. ISSN: 1473-7116. DOI: [10.1017/s0263593300006301](https://doi.org/10.1017/s0263593300006301).
- Zeebe, R. E., J. C. Zachos, and G. R. Dickens (2009). "Carbon dioxide forcing alone insufficient to explain Palaeocene–Eocene Thermal Maximum warming". *Nature Geoscience* 2(8), pages 576–580. DOI: [10.1038/ngeo578](https://doi.org/10.1038/ngeo578).